JGR Biogeosciences

RESEARCH ARTICLE
10.1029/2020JG005880

Key Points:

- The carbon turnover time in soil (τ_{soil}) has a higher climate sensitivity to temperature and precipitation than that of biomass (τ_{veg})
- The strong climate responses of woody allocation and soil decomposition in combination contribute to the higher climate sensitivity of τ_{soil} than τ_{veg}
- The higher climate sensitivity of τ_{soil} than τ_{veg} led to a decreased soil carbon sequestration capacity under warm and humid conditions

Supporting Information:

Supporting Information may be found in the online version of this article.

Correspondence to:

H. He and L. Zhang,
hehl@igsnrr.ac.cn;
li.zhang@igsnrr.ac.cn

Citation:

Ge, R., He, H., Zhang, L., Ren, X., Williams, M., Yu, G., et al. (2022). Climate sensitivities of carbon turnover times in soil and vegetation: Understanding their effects on forest carbon sequestration. *Journal of Geophysical Research: Biogeosciences*, *127*, e2020JG005880. https://doi.org/10.1029/2020JG005880

Received 3 NOV 2020
Accepted 4 FEB 2022

Climate Sensitivities of Carbon Turnover Times in Soil and Vegetation: Understanding Their Effects on Forest Carbon Sequestration

Rong Ge[1,2,3], Honglin He[1,4,5], Li Zhang[1,4], Xiaoli Ren[1,4], Mathew Williams[6], Guirui Yu[1], T. Luke Smallman[6], Tao Zhou[7], Pan Li[8], Zongqiang Xie[9], Silong Wang[10], Huimin Wang[1], Guoyi Zhou[11], Qibin Zhang[9], Anzhi Wang[10], Zexin Fan[12], Yiping Zhang[12], Weijun Shen[11], Huajun Yin[13], and Luxiang Lin[12]

[1]Key Laboratory of Ecosystem Network Observation and Modeling, Institute of Geographic Sciences and Natural Resources Research, Chinese Academy of Sciences, Beijing, China, [2]School of Government Audit, Institute of Natural Resources and Environmental Audits, Nanjing Audit University, Nanjing, China, [3]University of Chinese Academy of Sciences, Beijing, China, [4]Institute of Geographic Sciences and Natural Resources Research, National Ecosystem Science Data Center, Chinese Academy of Sciences, Beijing, China, [5]College of Resources and Environment, University of Chinese Academy of Sciences, Beijing, China, [6]School of GeoSciences and National Centre for Earth Observation, University of Edinburgh, Edinburgh, UK, [7]State Key Laboratory of Earth Surface Processes and Resource Ecology, Beijing Normal University, Beijing, China, [8]Institute of Surface-Earth System Science, Tianjin University, Tianjin, China, [9]State Key Laboratory of Vegetation and Environmental Change, Institute of Botany, Chinese Academy of Sciences, Beijing, China, [10]Institute of Applied Ecology, Chinese Academy of Sciences, Shenyang, China, [11]South China Botanical Garden, Chinese Academy of Sciences, Guangzhou, China, [12]Key Laboratory of Tropical Forest Ecology, Xishuangbanna Tropical Botanical Garden, Chinese Academy of Sciences, Mengla, China, [13]Chengdu Institute of Biology, Chinese Academy of Sciences, Chengdu, China

Abstract

The high uncertainty associated with the response of terrestrial carbon (C) cycle to climate is dominated by ecosystem C turnover time (τ_{eco}). Although the relationship between τ_{eco} and climate has been extensively studied, significant knowledge gaps remain regarding the differential climate sensitivities of turnover time in major biomass (τ_{veg}) and soil (τ_{soil}) pools, and their effects on vegetation and soil C sequestration under climate change are poorly understood. Here, we collected multiple time series observations on soil and vegetation C from permanent plots in 10 Chinese forests and used model-data fusion to retrieve key C cycle process parameters that regulate τ_{soil} and τ_{veg}. Our analysis showed that τ_{veg} and τ_{soil} both decreased with increasing temperature and precipitation, and τ_{soil} was more than twice as sensitive (1.27 years/°C, 1.70 years/100 mm) than τ_{veg} (0.53 years/°C, 0.40 years/100 mm). The higher climate sensitivity of τ_{soil} caused a more rapid decrease in τ_{soil} than in τ_{veg} with increasing temperature and precipitation, thereby significantly reducing the difference between τ_{soil} and τ_{veg} (τ_{diff}) under warm and humid conditions. τ_{diff}, an indicator of the balance between the soil C input and exit rate, was strongly responsible for the variation (more than 50%) in soil C sequestration. Therefore, a smaller τ_{diff} under warm and humid conditions suggests a relatively lower contribution from soil C sequestration. This information has strong implications for understanding forest C-climate feedback, predicting forest C sink distributions in soil and vegetation under climate change, and implementing C mitigation policies in forest plantations or soil conservation.

Plain Language Summary

Carbon turnover time is the average time that a carbon atom stays in an ecosystem from entrance to exit. Together, ecosystem carbon input via photosynthesis (i.e., productivity) and carbon turnover time determine ecosystem carbon sequestration. However, in contrast to the well-studied ecosystem productivity, carbon turnover time was found to dominate the uncertainty in terrestrial carbon sequestration and its response to climate. However, the climate sensitivities of carbon turnover times in various plant and soil pools and their effects on carbon storage have not been well-studied. Here, we quantified that carbon turnover time in soil (τ_{soil}) was more sensitive to climate than that of vegetation (τ_{veg}). This finding indicated the difference between τ_{veg} and τ_{soil} (τ_{diff}) being shortened in warm and humid regions. We further found that τ_{diff}, as an indicator of the balance between soil carbon input and the carbon exit rate, is closely associated with the capacity for soil carbon sequestration. Therefore, a decreasing τ_{diff} with increasing temperature/precipitation indicates a smaller proportion of carbon sequestered by soil than vegetation. Our findings facilitate understanding of carbon-climate feedback and the prediction of carbon sink distributions

under climate change and could guide the implementation of carbon mitigation policies for vegetation/soil conservation.

1. Introduction

The ways in which terrestrial carbon (C) storage responds to climate arguably represents the greatest uncertainty in predicting the future global C sink (Friedlingstein et al., 2014). Gross primary productivity (GPP, C influx to enter the ecosystem) and C turnover time (time taken for C to exit the ecosystem) are two key determinants of terrestrial C sequestration (Luo et al., 2017). However, relative to the well-studied and strongly converged modeling of GPP, the ecosystem C turnover time has been found to dominate the uncertainty in the response of terrestrial C sequestration to future climate change (Friend et al., 2014; He et al., 2016; Luo et al., 2017; Todd-Brown et al., 2013). Therefore, it is important to quantify terrestrial C turnover time and climate sensitivity accurately to understand the climate-C cycle feedbacks and reduce the predictive uncertainty.

Terrestrial C turnover is determined by both biotic and abiotic factors (Luo et al., 2003). Numerous studies have suggested that the terrestrial C turnover time is closely linked to climate factors, such as temperature and precipitation (Carvalhais et al., 2014; Chen et al., 2013; Knorr et al., 2005). For example, Carvalhais et al. (2014) found a negative correlation between temperature and ecosystem C turnover time (τ_{eco}) across most regions worldwide. However, the τ_{eco} emerges from multiple ecosystem C compartments that vary greatly in their individual turnover times (Bloom et al., 2016; Malhi et al., 2009); leaf, root, and wood turnover and plant mortality in live biomass, as well as litter and soil C decomposition in dead organic C pools, are all key processes that collectively regulate the τ_{eco} and its covariation with climate (Sitch et al., 2003; Trumbore, 2000, 2006). Previous studies have primarily been focused on the τ_{eco} or soil turnover time (τ_{soil}; Heckman et al., 2014; Koven et al., 2015; Schimel et al., 1994) because soil is usually the largest C pool in terrestrial ecosystems and has a longer turnover time than vegetation (Schmidt et al., 2011). The sixfold underestimation of the τ_{soil} in land surface models (LSMs) directly led to the soil C sequestration potential being overestimated by a factor of nearly two (He et al., 2016). By contrast, the vegetation C turnover time (τ_{veg}) has been examined less frequently, although it is a crucial process in regulating C cycling (Erb et al., 2016) and an essential parameter in C cycle models to predict the biomass allocation and productivity of an ecosystem (Fox et al., 2009; Thurner et al., 2017; Xia et al., 2015; Xue et al., 2017).

Recently, several studies have separated the τ_{eco} into the τ_{soil} and τ_{veg} to analyze their spatial patterns, correlations with climate, and effects on C sequestration (Bloom et al., 2016; Koven et al., 2015; Wang et al., 2018; Wu et al., 2018; Yan et al., 2017). For example, Bloom et al. (2016) retrieved the global terrestrial C turnover times via model-data fusion (MDF) analysis and suggested a contrasting spatial feature between the τ_{soil} and τ_{veg}. Wang et al. (2018) combined an analysis of the vegetation biomass, soil organic C stock, and flux observations to reveal that the τ_{soil} and τ_{veg} have different climatic and biotic controlling factors. Koven et al. (2015) analyzed Coupled Model Intercomparison Project Phase 5 (CMIP5) simulations and determined which changes in vegetation/soil pools were controlled more by productivity or τ_{veg}/τ_{soil}-driven changes. However, few studies have quantified the climate sensitivity of turnover times, which is directly associated with the responses of ecosystem C sinks to climate change (Friend et al., 2014). Wu et al. (2018) modeled the climate sensitivities of both biomass and soil C turnover times separately, but observational data sets were used only for evaluating the model performance and not for comparing climate sensitivities between turnover times of biomass and soil C pools. Therefore, despite the expectation that the τ_{veg} (vegetation C exit rate) and τ_{soil} (soil C exit rate) should have different physiological processes and climate responses (Bradford et al., 2016; De Kauwe et al., 2014), we still know little about how they differ in their sensitivities to climate and how these differences affect ecosystem C sequestration. As the temperature sensitivity of vegetation/soil C exit processes (e.g., for respiration (Q_{10})) has become a hotly debated topic in its variability and heterogeneous (Conant et al., 2011; Mahecha et al., 2010; Meyer et al., 2018; Zhou et al., 2009), a deeper understanding of the climate sensitivities of τ_{veg} and τ_{soil} and their potential mechanisms is imperative to accurately predict C sinks and their feedbacks to climate.

In this study, we examined the difference in climate sensitivity between the τ_{veg} and τ_{soil}, the underlying mechanism, and the effect of this difference on ecosystem C sequestration. We hypothesized that τ_{veg} has a lower climate sensitivity than τ_{soil}. The rationale for this hypothesis is that τ_{veg} is more dependent on the combined effects of the vegetation type and land use compared to soil and climate factors and is dominated by vegetation age (Erb et al., 2016; Wang et al., 2018, 2019). To test this hypothesis, long-term dynamic observational data of

soil, vegetation, and climate were collected from 10 forest sites in eastern China. These forests represent a large, globally important C sink (362 ± 39 g C m^{-2} yr^{-1}, mean ± 1 SE) that is affected by the eastern Asia monsoon and is characterized by high nitrogen deposition and a young age structure (Yu et al., 2014); most typical forest types in the Northern Hemisphere (e.g., cold-temperate coniferous forest, temperate coniferous and broad-leaved mixed forest, warm temperate deciduous broad-leaved forest, subtropical evergreen broad-leaved forest, and tropical monsoon rainforest) can be found here (Fu et al., 2010). Although we collected multitype observations, these observations only cover partial information related to the soil or vegetation C dynamics in the ecosystem and therefore cannot be used to estimate τ_{veg} and τ_{soil} directly. The MDF method is an effective approach to retrieving and optimizing key C cycle states and process parameters that cannot be obtained solely from observations while still being necessary for turnover time estimation; moreover, the MDF can quantify the realistic dynamic disequilibrium state of the terrestrial C turnover times, because it assimilates multiple sources of time series information from field observations into process-based models (Bloom et al., 2016; Zhou et al., 2013). Thus far, MDF has been widely applied to turnover time estimations across global scales (Ge et al., 2019; Luo et al., 2003; Zhang et al., 2010; Zhou et al., 2012). Here, the observed dynamic data were integrated with an intermediate complexity C cycle model (Data Assimilation Linked Ecosystem Carbon, DALEC; Bloom & Williams, 2015; Williams et al., 2005) based on MDF. Then, we retrieved the key parameters related to C allocation and turnover processes that regulate vegetation and the soil C cycle at a dynamic disequilibrium state. These parameters help to explain the different climate sensitivities between τ_{soil} and τ_{veg} in a transparent way. The difference in climate sensitivities of τ_{veg} and τ_{soil} can be expected to cause a difference between the τ_{veg} and τ_{soil} (τ_{diff}) under climate change. We then quantified how τ_{diff}, as an indicator of the balance between the vegetation C exit rate (equal to the soil C input rate) and the soil C exit rate, acts on soil C sequestration. The objectives of this study were to (a) quantify the magnitudes of τ_{veg} and τ_{soil} and their spatial patterns; (b) investigate the differences in the responses of τ_{veg} and τ_{soil} to climate, test the hypothesis, and explore the underlying mechanisms based on the optimized process parameters; and (c) reveal the effects of differences in the climate sensitivities of τ_{veg} and τ_{soil} on τ_{diff} and ecosystem C sequestration.

2. Materials and Methods

2.1. Site Description

Ten sites in the Chinese Ecosystem Research Network (CERN) with long-term observation data were selected that encompass typical forest types in China, including tropical rainforest, subtropical evergreen coniferous and broad-leaved mixed forest, warm temperate deciduous broad-leaved forest, and temperate coniferous and broad-leaved forest (Figure 1). The sites span precipitation and temperature gradients from south to north. Across the 10 sites, the latitude ranged from 22°N to 42°N, the forest age ranged from 30 to 400 years old, the mean annual temperature ranged from 3.6 to 22.6°C, and the mean annual precipitation ranged from 427 to 1,669 mm. Of the different regions, the Xishuangbanna tropical seasonal rainforest (BNF), Dinghu Mountain subtropical evergreen coniferous and broad-leaved mixed forest (DHF), Ailao Mountain subtropical evergreen broad-leaved forest (ALF), and Changbai Mountain temperate deciduous coniferous and broad-leaved mixed forest (CBF) are mature natural forests; Shennongjia subtropical evergreen deciduous broad-leaved mixed forest (SNF) and Huitong subtropical evergreen broad-leaved forest (HTF) are natural secondary forests; and other sites, that is, Beijing warm temperate deciduous broad-leaved mixed forest (BJF), Maoxian warm temperate deciduous coniferous mixed forest (MXF), Qianyanzhou subtropical evergreen artificial coniferous mixed forest (QYF), and Heshan subtropical evergreen broad-leaved forest (HSF), are plantations of middle-aged and young forests. All the sites are well protected, with little deforestation and other disturbances from human activities. Details regarding the vegetation, soil, climate, and geographic characteristics of each permanent plot can be found in Table S1 in Supporting Information S1.

2.2. Data

We applied daily observations of some meteorological parameters (i.e., daily max air temperature (T_{max}), daily min air temperature (T_{min}), daily average air temperature (T), global radiation (Rg), photosynthetically active radiation (PAR), precipitation (PRCP), and vapor pressure deficit (VPD)) and constant soil parameters (soil textural information indicating the soil, sand, and clay percentages) to drive the model of the 10 sites from 2005 to 2015. Furthermore, the C state and process variables were constrained by eight data sets from at each site, including

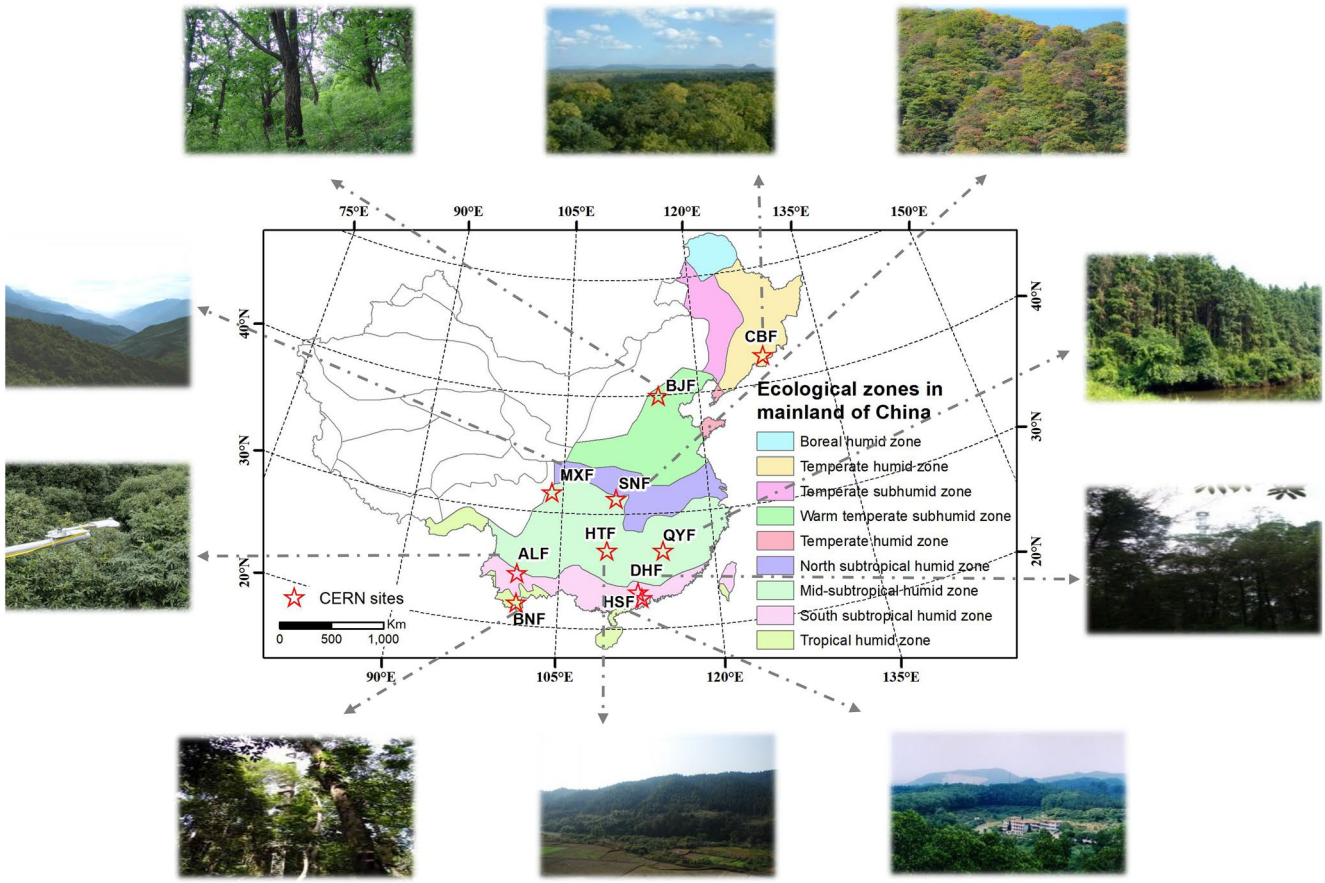

Figure 1. Map showing the distribution of 10 forest ecosystems in the Chinese Ecosystem Research Network (CERN). BNF: Xishuangbanna tropical seasonal rainforest; HSF: Heshan subtropical evergreen broad-leaved forest; DHF: Dinghu Mountain subtropical evergreen coniferous and broad-leaved mixed forest; ALF: Ailao subtropical evergreen broad-leaved forest; QYF: Qianyanzhou subtropical evergreen artificial coniferous mixed forest; HTF: Huitong subtropical evergreen broad-leaved forest; SNF: Shennongjia subtropical evergreen deciduous broad-leaved mixed forest; MXF: Maoxian warm temperate deciduous coniferous mixed forest; BJF: Beijing warm temperate deciduous broad-leaved mixed forest; CBF: Changbai Mountain temperate deciduous coniferous and broad-leaved mixed forest.

three biomass data sets (biomasses of foliage, fine roots, and wood) and a soil organic C (SOC) data set of observations performed at least once every 5 years from 2005 to 2015, a canopy dynamic data set (of seasonal leaf area index (LAI) measured at least quarterly every year), an annual litterfall data set, and two flux data sets (on the daily net ecosystem exchange (NEE) and monthly soil respiration (R_s)). The meteorological drivers, biomass, SOC, and LAI constraint data were all obtained from the CERN scientific and technological resources service system (http://www.cnern.org.cn/). The flux-tower NEE data used in this study were obtained at ChinaFLUX (http://www.chinaflux.org/general/). The R_s data were measured using static chamber-gas chromatography techniques and provided by Zheng et al. (2010). Details on the observational period and numbers for each data set can be found in Table S2 in Supporting Information S1.

2.3. Multiple Data-Model Fusion at the Dynamic Disequilibrium State

In a realistic dynamic disequilibrium state, C pools vary dynamically over time (i.e., $dC/dt \neq 0$); thus, long-term and dynamic observations of C stocks and fluxes were used to constrain and parameterize the DALEC model at a nonsteady state (Equation 1) independently at each site. To test whether these parameters are overfitted, we also did a fivefold cross-validation experiment; specifically, in each fold, 20% of observed data were removed randomly and unrepeatably to implement assimilation during each site, in contrast to all-data assimilation. Regarding the initial states of the C pools, usually they are determined by a spin-up run of the model, which iterating hundred to thousand years to achieve the steady state to initialize the C pools. However, to avoid the uncertainty arising from the steady state assumption in spin-up process (Carvalhais et al., 2008, 2010; Exbrayat

et al., 2014), here the initial states of the C pools were determined by the first available observation of C stocks or optimized (i.e., the labile pool, which cannot be directly observed). Then, the optimized parameter sets were used in forward modeling driven by the dynamic environmental variables to estimate the turnover times and C sequestration in soil, vegetation, and the whole ecosystem.

$$\begin{cases} \dfrac{dC}{dt} \neq 0 \\ C_i(t+1) = C_i(t) + I_i(t) - \ k_i C_i(t), \quad i = 1, 2, \ldots, n \\ C_i(t=0) = \ C_i 0 \end{cases} \tag{1}$$

where C_i, I_i, and k_i represent the size, input, and turnover rate of the ith C reservoir, respectively, and $C_i 0$ represents the initial state of the ith C reservoir.

Specifically, we used the latest version of DALEC (Famiglietti et al., 2021; Smallman et al., 2017), which is an intermediate-complexity model that has been improved in terms of its number of dead C pools and process representations related to photosynthesis, decomposition regulated by both temperature and soil moisture, and water cycle feedbacks (Figure S1 in Supporting Information S1). The C cycle was initiated with the canopy C influx: gross primary productivity (GPP), which was predicted using the aggregated canopy model (ACM-GPP-ET; Smallman & Williams, 2019). There is a strong coupling between C cycle and water cycle processes, and it is mediated directly by stomatal conductance and indirectly by the root zone soil moisture content and its accessibility. ACM-GPP-ET is a simple aggregated set of equations operating on the LAI (determined directly from foliage pool), total daily irradiance, minimum and maximum daily temperature, day length, water potential gradient, and total soil-plant hydraulic resistance. After GPP is consumed in a specific fraction (f_{auto}) by autotrophic respiration (R_{a}), the remaining photosynthate (NPP) is allocated to plant tissue pools (foliar, labile, wood, and fine roots). The degraded C from these plant tissue pools then goes to two dead organic matter pools (litter and soil) with heterotrophic respiration (R_{h}) losses. The C exiting from all the C reservoirs was based on a first-order differential equation with various turnover rates, with temperature and moisture dependency on the turnover from the litter and soil pools.

In this version, the DALEC model includes a multilayer representation of the soil and root access (Smallman & Williams, 2019). There are five soil layers, three of which are accessible to roots to supply the canopy with water. The top two layers have a fixed thickness of 10 and 20 cm, with a third layer that is expandable based on root penetration. The soil layer-specific field capacity, porosity, and hydraulic conductances are calculated using the soil texture. Using these data, infiltration by precipitation, drainage between soil layers, soil hydraulic resistance to root uptake of water, and soil surface evaporation are estimated. Therefore, we added a decomposition response that was linked to the soil moisture content of the topsoil layer. In contrast to the original DALEC version that considered only the temperature dependency, here, we added a moisture scalar to the litter and soil decomposition process since the R_{h} process is both temperature-sensitive and soil moisture-sensitive. The detailed exponential response equation from Sierra et al. (2015) is as follows, which improved the model structure to quantify the climatic sensitivity of turnover times to both temperature and moisture factors equally. The R_{h} includes a fine litter pool ($R_{\text{h\_lit}}$ composed of foliar and fine root inputs), wood litter ($R_{\text{h\_woodlit}}$ composed of both fine and coarse woody debris), and soil organic matter ($R_{\text{h\_som}}$). Decomposition and mineralization follow a first-order kinetic approach with environmental modifiers. When litter and wood litter pools turn over, a fraction of their C is released as heterotrophically respired C, while the remainder passes to the soil organic matter pool (D_{lit}, D_{litwood}; $\text{gC m}^{-2}\ \text{d}^{-1}$). All decompositions of soil organic matter are heterotrophically respired as CO_2. R_{h} follows first-order kinetics with exponential temperature sensitivity and exponential soil moisture sensitivity.

$$R_{\text{h\_lit}} = C_{\text{lit}} \times \theta_{\text{lit}} \times f_{\text{T}} \times f_{\text{w}} \tag{2}$$

$$R_{\text{h\_som}} = C_{\text{som}} \times \theta_{\text{som}} \times f_{\text{T}} \times f_{\text{w}} \tag{3}$$

$$R_{\text{h\_woodlit}} = C_{\text{woodlit}} \times \theta_{\text{woodlit}} \times f_{\text{T}} \times f_{\text{w}} \tag{4}$$

$$f_{\text{T}} = 0.5 e^{Rh_{\text{temp}} \times T} \tag{5}$$

$$f_{\text{w}} = e^{-e^{(a - b \times SWC)}} \tag{6}$$

where R_{h_lit}, R_{h_som}, and $R_{h\_woodlit}$ refer to the heterotrophic respiration from foliar and fine root litter (C_{lit}), soil organic matter pools (C_{som}), and both fine and coarse woody debris ($C_{woodlit}$), respectively; θ_{lit}, θ_{som}, and $\theta_{woodlit}$ refer to the baseline turnover rates of the C_{lit}, C_{som}, and $C_{woodlit}$ pools; f_T and f_w refer to the temperature and moisture scalars to adjust the real turnover rate, respectively; T is the daily air temperature; Rh_{temp} is the heterotrophic respiration exponential temperature dependence; SWC is the daily soil water content at 0–10 cm; and a, b are adjustment constants.

The C pools and fluxes in the DALEC were iteratively calculated at a daily time step and determined as a function of the key turnover and allocation parameters (Table S3 in Supporting Information S1). The Metropolis simulated annealing algorithm, a variation of the Markov chain Monte Carlo (MCMC) technique, was applied to optimize the model parameters (Hurtt & Armstrong, 1996; Metropolis et al., 1953). Moreover, we imposed a sequence of ecological and dynamic constraints (EDCs) on the model parameters and pool dynamics to improve the MDF performance further (Bloom et al., 2016; Bloom & Williams, 2015; Smallman et al., 2017), which can significantly reduce uncertainty (34%) in model parameters and simulations. A detailed description of the dynamic disequilibrium method can be found in our previous study (Ge et al., 2019).

2.4. Estimation of Turnover Time, Climate Sensitivity, and C Sequestration

At a realistic dynamic disequilibrium state, τ was defined as the ratio between the mass of a C pool and its outgoing fluxes (Schwartz, 1979). Note that because there were few natural and anthropogenic disturbances at these well-protected CERN sites (Zhang et al., 2010; Zhou et al., 2006), the C efflux was approximately equivalent to the heterotrophic respiration (R_h) for the soil pool and the sum of autotrophic respiration (R_a) and litterfall (plant mortality) for the vegetation pool. Hence, the turnover times for vegetation, soil, and the whole ecosystem were derived as follows:

$$\tau_{veg} = \frac{C_{live}}{I_{live} - \Delta C_{live}} = \frac{C_{live}}{\text{litterfall} + R_a} \tag{7}$$

$$\tau_{soil} = \frac{C_{dead}}{I_{dead} - \Delta C_{dead}} = \frac{C_{dead}}{R_h} \tag{8}$$

$$\tau_{eco} = \frac{C_{eco}}{I_{eco} - \Delta C_{eco}} = \frac{C_{dead+}C_{live}}{R_h + R_a} \tag{9}$$

where C_{live}, C_{dead}, and C_{eco} refer to the live biomass C pool size (C_f, C_r, and C_w), dead organic C pool size (C_{soil} and C_{litter}), and whole ecosystem C pool size, respectively; I_{live}, I_{dead}, and I_{eco} refer to the C input into the live biomass C pool, dead organic C pool, and whole ecosystem C pool, respectively; ΔC_{live}, ΔC_{dead}, and ΔC_{eco} refer to changes in the live biomass C pool, dead organic C pool, and whole ecosystem C pool, respectively; and R_a and R_h refer to the autotrophic and heterotrophic respiration, respectively, which were all calculated from the DALEC output driven by the optimized parameters and dynamic meteorological drivers. The C reservoirs, fluxes, and turnover times are instantaneous values. Here, we used the yearly turnover times from 2005 to 2015 and the mean annual value at each site to determine their climate sensitivity under climate change and various climatic conditions.

We estimated the responses of the τ_{veg} and τ_{soil} to climate variables using a simple linear regression approach:

$$\tau = aX_T + \varepsilon_T \tag{10}$$

$$\tau = bX_{PRCP} + \varepsilon_{PRCP} \tag{11}$$

where τ is the estimated turnover time for vegetation or soil, and X_T and X_{PRCP} are the mean annual temperature and precipitation, respectively. The regression coefficients a and b represent the sensitivities of the C turnover times to two climate variables across the 10 sites, and ε_T and ε_{PRCP} are the corresponding residual errors.

The optimized parameter values and the initial observations of the corresponding C pool sizes were used in forward modeling driven by the dynamic environmental variables from 2005 to 2015 (Zhou & Luo, 2008). The net ecosystem productivity (NEP) was further derived from the difference between the modeled ecosystem C influx GPP and C outgoing fluxes ($R_a + R_h$). To further analyze the effect of difference in the climate sensitivities

of τ_{veg} and τ_{soil} on forest ecosystem C sequestration, we then split the NEP into C sinks sequestered in dead organic C pools, which were calculated as the C stock changes in the soil and litter pools (ΔC_{dead}).

2.5. Comparison With Assimilated Benchmark and LSM Simulations

We chose the globally estimated turnover times by using the CARbon DAta MOdel framework (CARDAMOM; Bloom et al., 2016) as an assimilated benchmark and TRENDY v6 (Le Quéré et al., 2018; Sitch et al., 2015) as simulations from most state-of-the-art LSMs. All regional pixels of the two products in the Northern Hemisphere were calculated to compare with our MDF results from the typical forest sites across the Northern Hemisphere. Specifically, CARADAMOM was driven by monthly time steps from European Centre for Medium-Range Weather Forecasts (ECMWF) Reanalysis Interim (ERA-interim) meteorology data sets and the MODIS burned area product at a $1° \times 1°$ resolution for the 2005–2015 period. The global observational constraints consisted of MODIS LAI, vegetation biomass (Carvalhais et al., 2014), and the Harmonized World Soil Database (HWSD) SOC stocks, which were all assimilated into DALEC in this framework to retrieve the τ_{veg} and τ_{soil}.

The LSM τ estimations were generated from simulated vegetation, soil C stocks and fluxes by a set of 13 LSMs (i.e., OCN, CABLE, CLASS, CLM, DLEM, ISAM, LPJ-WSL, LPJ-GUESS, LPX, ORCHIDEE, ORCHIDEE-MICT, VEGAS, and VISIT; Table S4 in Supporting Information S1) from the recent TRENDY v6 intercomparison project in which models are forced with changing climate, CO_2, and LULCC (S3 experiments) for the 2005–2015 period. Specifically, for τ_{veg}, since the vegetation efflux was not processed as an output in TRENDY (e.g., litterfall), we estimated the τ_{veg} using $dC_{veg}/dt = \mathrm{GPP} - C_{veg}/\tau_{veg}$, which was used to indirectly calculate the difference between annual vegetation C stock variation and GPP as vegetation efflux, while we directly calculated the τ_{soil} using the and soil efflux $Rh = C_{soil}/\tau_{soil}$.

3. Results

3.1. Performance of Model Simulations

The modeled biometric and soil variables were consistent with the observational data for the corresponding eight variables, with the scatter points aligning with the 1:1 line (Figures 2a–2h). Specifically, the determination coefficients (R^2) for the C stock-related variables varied from 0.94 to 0.99, and the root-mean-square errors (RMSEs) were small relative to their magnitudes (Figures 2a–2e). By contrast, the R^2 values for the C fluxes (NEE, Rs, and litterfall) were slightly lower (0.60–0.65, Figures 2f–2h), but the bias values were within 1 standard deviation of the observations. In addition, the optimized parameters were well constrained by multiple and long-term observations; the standard deviations of the retrieved parameters were typically <35% of the mean parameter values (Figure S2 in Supporting Information S1). The litter decomposition coefficient, θ_{min}, was an exception, with a standard deviation of 85% of the mean parameter estimate (Figure S2g in Supporting Information S1). High uncertainty associated with belowground processes was not unexpected, because the only incorporated information on belowground processes was soil respiration and soil C storage. According to a fivefold cross validation, the accuracy of the C flux and pool simulations were close to those in the all-data assimilation (Figure S4 in Supporting Information S1), so the random lack of constraint data did not impact the assimilation, and these parameters were not overfitted.

3.2. Estimated τ_{soil} and τ_{veg} and Their Climate Sensitivities

The mean annual τ_{veg} ranged from 3.8 to 19.3 years (mean 10.5 years), whereas the τ_{soil} ranged from 12.9 to 51.6 years (mean 29.8 years), and the τ_{eco} ranged from 8.8 to 35.9 years (mean 22.2 years) at the 10 sites (Figure 3a). The τ_{soil} was more than twice that of the τ_{veg} in the 10 typical forest ecosystems, which was attributed primarily to the slower rate of C decomposition in the soil pools than that of the plant tissues (Figures S2d–S2i in Supporting Information S1). Moreover, the τ_{soil} dominated the magnitude and pattern of the τ_{eco} and explained more than 70% of the variance in the τ_{eco} (Figure 3b).

The mean annual τ_{veg} and τ_{soil} across the 10 sites exhibited similar patterns, both of which were negatively correlated with the mean annual temperature and precipitation (Figures 3a and 3b). However, the sensitivity of the τ_{veg} to these two climatic variables was substantially lower than that of the τ_{soil}, which decreased from 1.27 to 0.53 years/°C (by 59%) for temperature and from 1.70 to 0.40 years/100 mm (by 81%) for precipitation

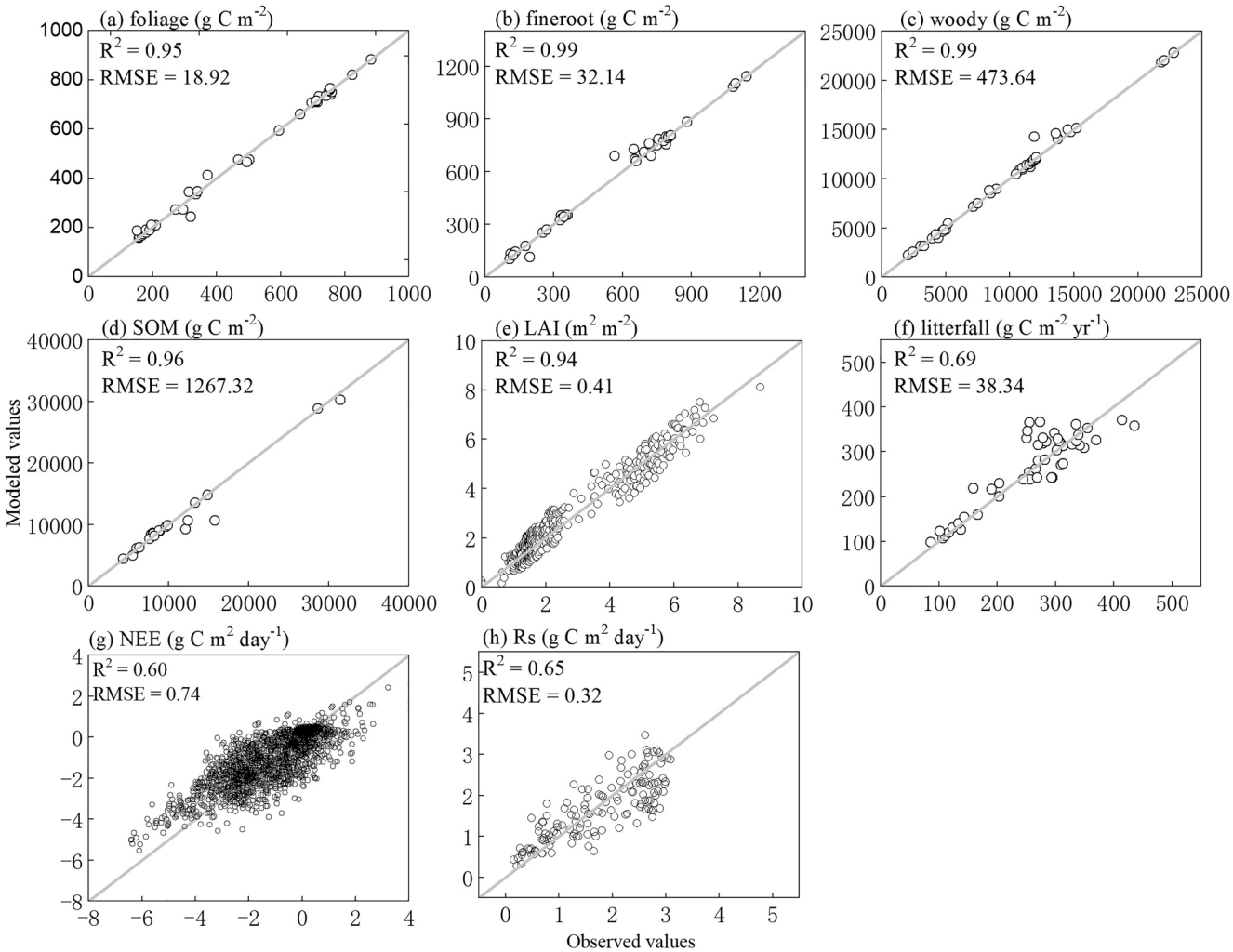

Figure 2. Performance of model-data fusion in C stock and flux estimations at all sites during the study period. For the scatterplots, the modeled values are plotted against observations to show the quality of the model fit.

(Figures 3a and 3b). Similarly, the annual time-varying τ_{veg} and τ_{soil} at each site indicated that the τ_{soil} has a more significant and higher climate sensitivity to varying temperatures than the τ_{veg} (Figures S7 and S10 in Supporting Information S1).

3.3. Key C Cycle Process Controls Over the Climate Sensitivities of τ_{soil} and τ_{veg}

3.3.1. Apparent C Stocks and Fluxes

The C turnover time is defined as the ratio of the C pool to its outgoing flux; therefore, the covariation in (a) vegetation C stocks, litterfall and R_a, as well as (b) soil C stocks and *Rh* with temperature and precipitation, were analyzed. The vegetation C stocks increased markedly with increasing temperature; although the correlation with precipitation was not statistically significant, the regression line also showed an obvious positive trend. By contrast, there were no significant trends for the soil C stocks (Figures 5a and 5b). R_a, R_h and litterfall both increased with increasing temperature and precipitation, although a statistically significant increase was observed only for the R_h and temperature. The R_h was more sensitive to climate variation than litterfall and R_a (Figures 5c and 5d). Overall, the fluxes had a higher variability than the C stocks and dominated the variation in C turnover time. Under rising temperatures, the significant increasing trend in the vegetation stocks and the nonsignificant increasing trend in litterfall and R_a formed two compensatory forces acting on the variation in the τ_{veg} (i.e., C_{veg}/(litterfall + R_a)), which resulted in a weaker slope of the τ_{veg} response to climate relative to that of τ_{soil} (Figure 4a).

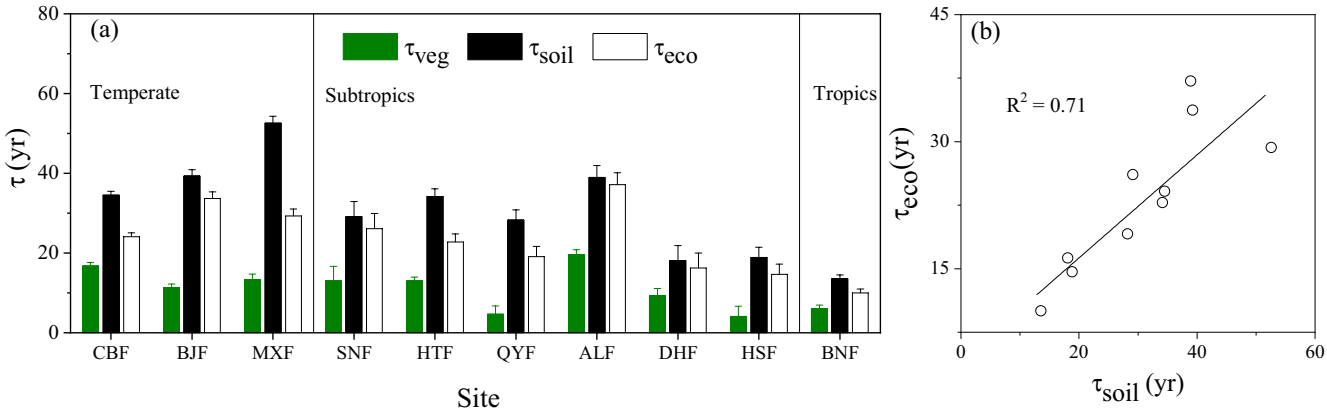

Figure 3. (a) Magnitude of C turnover time in the vegetation (τ_{veg}), soil (τ_{soil}), and whole ecosystem (τ_{eco}). The green, black, and white bars (mean value and 1 standard error (SE)) denote the τ_{veg}, τ_{soil}, and τ_{eco}, respectively. (b) There is a significant linear relationship between the τ_{soil} and τ_{eco}. Xishuangbanna tropical seasonal rainforest (BNF), Dinghu Mountain subtropical evergreen coniferous and broad-leaved mixed forest (DHF), Ailao Mountain subtropical evergreen broad-leaved forest (ALF), and Changbai Mountain temperate deciduous coniferous and broad-leaved mixed forest (CBF) are mature natural forests; Shennongjia subtropical evergreen deciduous broad-leaved mixed forest (SNF) and Huitong subtropical evergreen broad-leaved forest (HTF) are natural secondary forests. Other sites, that is, Beijing warm temperate deciduous broad-leaved mixed forest (BJF), Maoxian warm temperate deciduous coniferous mixed forest (MXF), Qianyanzhou subtropical evergreen artificial coniferous mixed forest (QYF), and Heshan subtropical evergreen broad-leaved forest (HSF), are plantations or middle-aged and young forests.

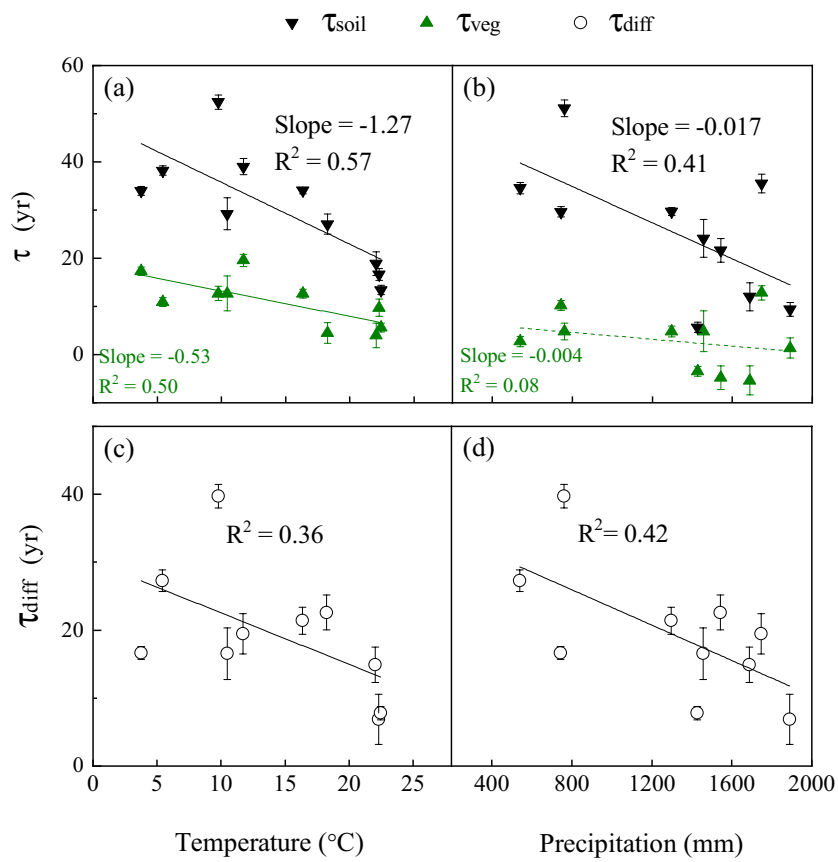

Figure 4. Associations of turnover times in vegetation (τ_{veg}) and soil (τ_{soil}) and their difference (τ_{diff}) (mean value and 1 SE) with the mean annual temperature (a), (c) and precipitation (b, d). The dashed and solid lines denote nonsignificant and significant regressions at the 0.05 level, respectively.

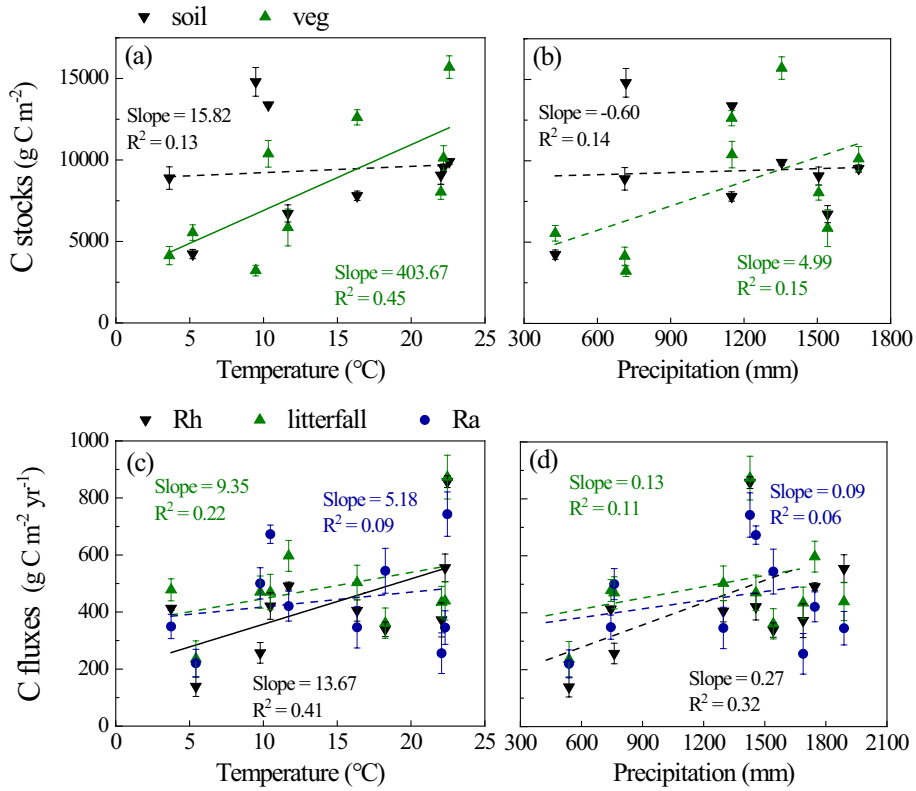

Figure 5. Associations of C pools (vegetation-green; soil-black) and fluxes in vegetation (litterfall and R_a) and soil (R_h) (mean value and 1 SE) with temperature (a, c) and precipitation (b, d). The dashed and solid lines denote nonsignificant and significant regressions, respectively. The ALF appears to be an outfitter with large vegetation and soil C pools (both more than 24,000 g C m^{-2}) among these sites due to its cold and wet conditions at high elevations (2,488 m); thus, this point was not incorporated into the linear regression in Figures 5a and 5b. The figure incorporated the ALF point into the linear regression can be found in Figure S6 in Supporting Information S1.

The lack of climate sensitivity in soil stocks together with the significant increasing trend of the R_h led to the higher sensitivity (greater slope in Figure 5a) of τ_{soil} (i.e., C_{soil}/R_h). The same pattern was supported by the available observations on soil and biomass C stocks and fluxes (i.e., litterfall and R_s), which verified the robustness of the simulated variation (Figure S5 in Supporting Information S1).

3.3.2. Underlying Parameters: Allocation and Turnover Rates

The C allocation and turnover among plant compartments as well as the decomposition of litter and soil are vital parameters that control C pools and fluxes and, thus, the τ_{veg} and τ_{soil}. Among the vegetation pools, we focused on woody allocation and turnover since woody tissue is the dominant pool of biomass and has a much longer turnover time than leaves and fine roots (Galbraith et al., 2013). Based on the regression of optimized parameters against climate data, we quantified the climate sensitivities of key parameters to explore why the τ_{soil} is more sensitive to climate than τ_{veg} (Figure 6). Their covariation with temperature is described as an example here (Figure 6a). We found that the decomposition rate in soil (θ_{som}) increased to a greater extent (2×10^{-6}/°C) than the wood mortality (θ_{woo}, 1×10^{-6}/°C) with increasing temperature; this trend caused the R_h to increase more rapidly than litterfall (13.67 g C m^{-2} yr^{-1}/°C versus 9.35 g C m^{-2} yr^{-1}/°C), resulting in a more rapid and significant decrease in τ_{soil} than in τ_{veg} (−1.27 years/°C versus −0.53 years/°C), which ultimately dominated the decrease in τ_{eco}. Since the soil C input (litterfall) and C output (R_h) both increased with temperature and precipitation, C_{soil} did not exhibit a pronounced sensitivity to climate (15.82 g C m^{-2}/°C); thus, C_{soil} had a negligible influence on the pattern of the τ_{soil} (i.e., C_{soil}/R_h), which was more affected by the R_h with high and significant climate sensitivity. Moreover, θ_{som}, rather than litter turnover (θ_{lit}), contributes more to the *Rh* variation and then dominates the climatic sensitivity of the whole dead organic C turnover time. Regarding the vegetation pools, the allocation to wood (f_{woo}) also increased with temperature and humidity. This rising f_{woo} significantly increased

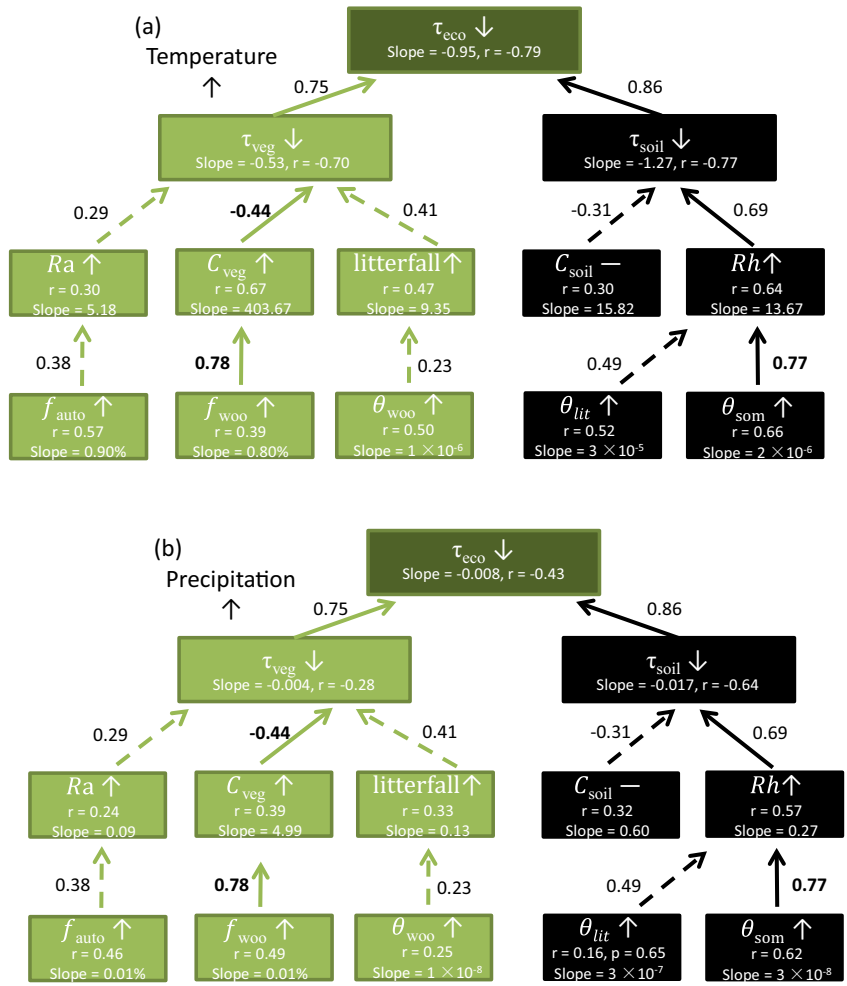

Figure 6. Dependencies of key process parameters in live biomass and dead organic matter on temperature (a) and precipitation (b) across sites. The boxes/lines denote processes in vegetation (green) and soil (black), where the *r* and slope in the boxes denote the correlation coefficient and sensitivity of these processes to varying temperature/precipitation. The arrows denote the nonsignificant (dashed) and significant (solid) effects of one process on another. The values next to the arrows denote the correlation coefficients between connected processes; negative values reflect negative effects.

the C_{veg} pool (403.67 g C m^{-2}/°C), while the rising f_{auto} and θ_{woo} increased autotrophic respiration and litterfall. The rising f_{woo} exerted a damping effect on the decline in τ_{veg} with increasing temperature and precipitation due to increasing plant mortality (θ_{woo}) and f_{auto}. Therefore, the sensitivity of τ_{veg} to both temperature and precipitation was much lower than that of τ_{soil}. Compared to climatic factors, biotic factors, that is, forest age, explained more of the variation in the τ_{veg} (61% in Figure 7a; temperature: 50%, and precipitation: 8% in Figures 4a and 4b). The dominant role of biotic factors (e.g., forest age) in controlling the τ_{veg} also contributed to the lower sensitivity of the τ_{veg} to climatic factors.

3.4. Effects of Climate Sensitivities of τ_{soil} and τ_{veg} on τ_{diff} and Ecosystem C Sinks

All 10 forests were net C sinks, with mean annual NEP values ranging from 244 to 445 g C m^{-2} yr^{-1} (Figure 8a) across sites. The ratio of C sinks in soil (ΔC_{dead}) to that in the whole ecosystem (NEP) varied from 18% to 68% across the 10 typical forests (Figures 8a and 8b). Moreover, 55% of this variation was explained by the difference between τ_{soil} and τ_{veg}, that is, τ_{diff} (Figure 8b, linear regression). Since τ_{veg} reflects the C input rate into the soil pool and τ_{soil} reflects the C exit rate from the soil pool, the difference in these two traits (τ_{diff}), as the balance of soil C input and exit rate, might largely explain the variation in the capacity for C sequestration in soil (Figure 8b). We found that the pattern and variation of τ_{diff} were determined by the various climate sensitivities of τ_{soil} and τ_{veg}. The

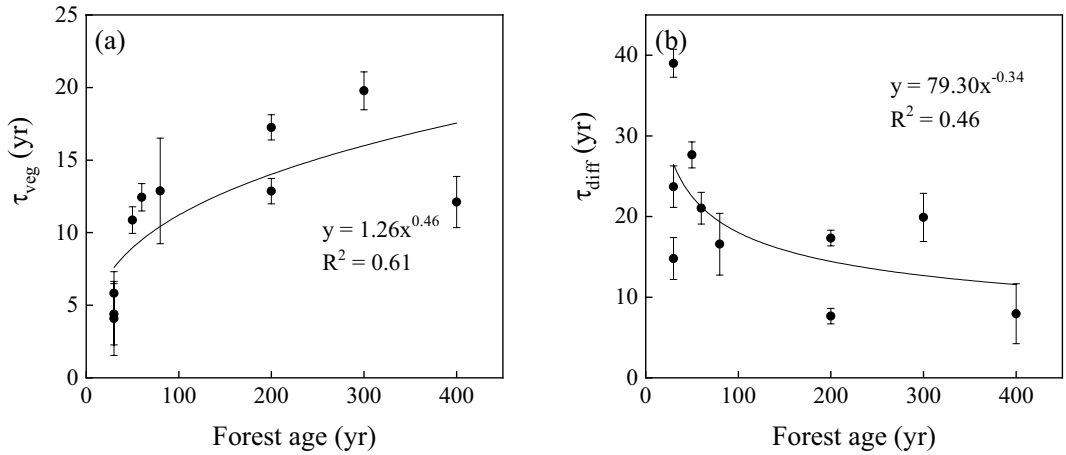

Figure 7. Correlations of vegetation turnover time (τ_{veg}, (a) and the difference between τ_{veg} and soil turnover time τ_{diff}), (b) (mean value and 1 SE) with forest age in the study sites across China. Power functions are fitted to the data, and their parameters and statistics are reported.

higher climate sensitivity of τ_{soil} than τ_{veg} led to more rapid decreases in τ_{soil} than τ_{veg} with increasing temperature and precipitation, thereby significantly decreasing the τ_{diff} under warm and humid conditions (Figures 4c and 4d). Accordingly, the lower τ_{diff} resulted in a significant decrease in the ratio of C sequestered in soil in warmer areas

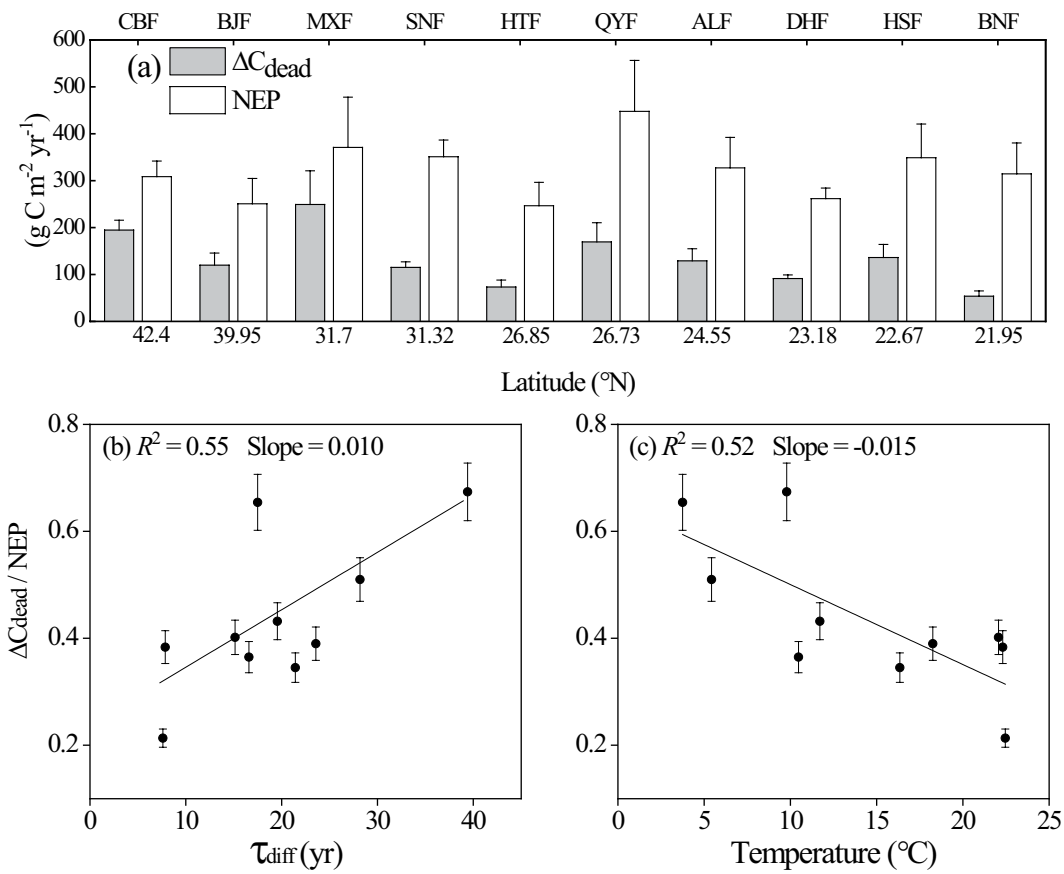

Figure 8. Magnitude (mean value and 1 SE) of C sinks fixed in soil (ΔC_{dead}) and in the whole ecosystem (NEP) across the latitudinal gradient of the 10 sites (a). Covariation of the ratio (mean value and 1 SE) of C sinks fixed in soil to that fixed in the whole ecosystem (ΔC_{dead} /NEP) with the differences between the turnover times in soil and vegetation (τ_{diff}) (b) and the mean annual temperature (c).

(Figure 8c). The detailed annually time-varying τ_{diff} and its covariation with temperature, as well as its effect on the ΔC_{dead} at each site, showed consistent patterns, further indicating that the decrease in τ_{diff} with climate warming led to a lower contribution of soil C sequestration (Figures S7 and S8 in Supporting Information S1).

4. Discussion

4.1. Estimation of Climate Sensitivity in τ_{veg}/τ_{soil} and Its Uncertainty

Various methods have been used to estimate C turnover times, for example, using the ratio of observed stocks and fluxes (e.g., Carvalhais et al., 2014; Yu et al., 2019), using model simulations (e.g., Wu, Piao et al., 2020; Zhou et al., 2013) or using MDF method (e.g., Zhang et al., 2010; Zhou et al., 2012). Direct observations cannot provide all the variables and parameters involved in estimating both vegetation and soil C turnover times, which are primarily dependent on process model simulations (Bloom et al., 2016; Koven et al., 2015; Yan et al., 2017). In contrast to the model simulation based on preset parameters, the applied MDF method facilitates the optimization of the model parameters and states according to the multiple and colocated observations on different soil and vegetation variables. It has long been a common practice in the ecological modeling community to calibrate parameters by fitting model outputs to observations via MDF, which has also been widely adopted and acknowledged in parameter inversion and C turnover time estimation for each specific site or each grid cell across large scales (Bloom et al., 2016; Ge et al., 2019; Luo et al., 2003; Zhang et al., 2010; Zhou et al., 2013). The advanced assimilation method, the collected prior information for parameters, and expert experiential knowledge used as model constraints (EDCs) can be adopted in MDF to ensure the optimized parameters have physiologically meaningful ranges and values and to avoid parameter overfitting effectively (Bloom & Williams, 2015; Smallman et al., 2017). These parameters, which cannot be solely obtained from observations, help to explain the underlying mechanism of climate sensitivities in τ_{soil} and τ_{veg} and then the C-climate feedback in a more transparent way in contrast to the apparent C stocks and fluxes. Moreover, MDF provides an effective approach to quantifying the realistic dynamic disequilibrium of the terrestrial C cycle, because it can assimilate long-term, time series and multiple observations into the process-based model (Bloom et al., 2016).

To improve the model predictive skill and reduce model uncertainty of turnover time estimation, improving model parameterization (via MDF) and increasing structural complexity (like Earth System Models (ESMs)) are two main approaches. The DALEC is an C cycle process model suitable for MDF with intermediate complexity. We still expect model structure improvement by including hypothesized missing C pools (e.g., adding numbers of dead organic C pools) or improving representations on over-simplified processes (e.g., fixed Ra:GPP fraction), or introducing additional processes (e.g., C-nitrogen cycling or C-water cycling). By contrast, the ESMs have high structure complexity, which can benefit not only long-term predictions of global change, but also near-term, regional-scale ecological forecasts aimed to inform sustainable decision making (Dietze et al., 2018; White et al., 2019) and modeling studies focused on understanding the recent past (Schwalm et al., 2020). However, the extent to which increased structural complexity can directly improve predictive skill is unclear (Famiglietti et al., 2021). It is therefore possible that other approaches to reducing C cycle model uncertainty (e.g., improving model parameterization via MDF) may be more effective than increasing structural realism in some circumstances (noted by Shiklomanov et al., 2020 and Wu, Cai, et al., 2020). On one hand, several recent ESM efforts have sought to enable the assimilation of eddy covariance or remote sensing observations on C pools (e.g., Norton et al., 2019; Peylin et al., 2016) as well as measurements of functional traits (e.g., LeBauer et al., 2013). The value of such efforts to reduce parameter uncertainty was underscored. On the other hand, the MDF models like DALEC with optimized parameters has comparable performance to state-of-art terrestrial biosphere model estimates in Trendy and CMIP5 (Quetin et al., 2020); recently, similar MDF-based model simulations were adopted as novel benchmark in the International Land Model Benchmarking (ILAMB) project on C cycle to evaluate and improve ESM performance (López-Blanco et al., 2019; Slevin et al., 2016).

Numerous studies have investigated the relationship between ecosystem turnover times and climate (e.g., Bloom et al., 2016; Carvalhais et al., 2014; Chen et al., 2013; Knorr et al., 2005; Wang et al., 2018; Yan et al., 2017), but few studies have quantified the different climatic sensitivities in the live and dead organic matter pools (e.g., Wu et al., 2018). Here, for the first time, we demonstrated quantitatively that the τ_{soil} was more sensitive to both temperature and precipitation than the τ_{veg}, and that the τ_{soil} dominated the response of the τ_{eco} to climate; furthermore, we revealed the underlying mechanism using optimized process parameters in a realistic disequilibrium state. In

comparison with previous studies on turnover times that have primarily been conducted under the steady state assumption (SSA), where C input is more easily obtained to estimate turnover time (e.g., Carvalhais et al., 2014; Yan et al., 2017), this retrieval is closer to reality against the background of global environmental changes (Bellassen et al., 2011; Luo & Weng, 2011). This nonsteady method effectively reduces the biases induced by SSA when estimating the initial states of C pools, C allocation and turnover coefficients (Carvalhais et al., 2008, 2010; Zhou et al., 2013), and it avoids underestimating turnover times and their sensitivities to climate in C sink regions (Ge et al., 2019). In addition, the optimized parameters (i.e., plant allocation, wood and root turnover, and soil decomposition) and the estimations for the τ_{veg} and τ_{soil} under dynamic disequilibrium all indicated high consistency with the existing empirical research based on field observations or experiments (Tables S5 and S6 in Supporting Information S1). Thus, our results provide reliable insight into the various climate sensitivities of τ_{veg} and τ_{soil}. Although soils in reality consist of C that turns over at different rates, ranging from fractions of a year to centuries, thus far, it has been challenging to separate soils into different pools and quantify each pool's turnover time through empirical studies due to a lack of corresponding observed data (Luo et al., 2016). When considering the various soil pools in simulation, even the state-of-art ESMs cannot accurately fit observations and are widely different in their projections of soil C dynamics (Todd-Brown et al., 2014; Yan et al., 2014). Our calculation implicitly assumes SOC as a single homogenous cohort, and estimates the average turnover time of C in the soil, which is called the apparent turnover time (Carvalhais et al., 2014). The approach is advantageous in representing the highly heterogeneous intrinsic properties of the terrestrial C cycle as an averaged apparent ecosystem property which is more intuitive to infer ecosystem-scale sensitivity of τ to climate change (Fan et al., 2020; Luo et al., 2019). Instead of focusing on the heterogeneity of individual compartment turnover times, we show the change in the C cycle on the ecosystem level using τ as an emergent diagnostic property.

4.2. Understanding the Mechanism of Higher Sensitivity of τ_{soil} Than of τ_{veg} to Climate

The higher climate sensitivity of τ_{soil} originated partly from the higher sensitivity of the soil C decomposition rate (θ_{som}) than of plant tissue mortality (e.g., the turnover rate of the largest vegetation pool, θ_{woo}). Empirical research has shown that the θ_{som} is highly dependent on soil temperature and moisture (Craine et al., 2010; Davidson & Janssens, 2006; Thomsen et al., 1999; Trumbore et al., 1996; Wang et al., 2018). By contrast, the responses of the θ_{woo} or plant mortality to climate remain largely uncertain (Smith et al., 2013). Many studies based on observations, experiments or modeling have suggested that there are weak to no relationships between the τ_{woo} (i.e., the inverse of θ_{woo}) and climate variables for tropical evergreen species (Galbraith et al., 2013; Malhi et al., 2004; Quesada et al., 2012). Other studies have suggested large increases in the θ_{woo} as the temperature increases, especially for temperate deciduous species (Adams et al., 2010, 2017; McDowell et al., 2016; Thurner et al., 2016; Williams et al., 2013). Climate-driven vegetation mortality usually occurs when there are extreme climatic events and related natural disturbances (e.g., drought, cold frost; Allen et al., 2010; Reichstein et al., 2013). Given this prior ecological knowledge, climate dependency was not represented in the θ_{woo} process in DALEC; this model structure could be expected to weaken the estimated climate sensitivity of the τ_{veg}.

In addition to θ_{woo}, allocation to wood (f_{woo}) is another key process that codetermines the τ_{veg}. The allocation among plant tissues has a clear relationship with climate, with a greater allocation to structural C (i.e., woody pools) with increasing temperature and precipitation (Figures S3a–S3c in Supporting Information S1 and Figures 6a, 6b; Bloom et al., 2016; Guillemot et al., 2015; Song et al., 2018; Xia et al., 2015). This relationship accounted for the distinct increase in vegetation stocks in the warmer and humid regions (Figures 5a and 5b). In addition, f_{auto} first decreased and then increased as the temperature increased at the turning point of approximately 11°C, which was in strong accordance with the synthetic analysis based on the global forest database and could be ascribed to the asymmetric response of RE and GPP to rising temperature (Piao et al., 2010). This positive response of the f_{woo} and f_{auto} to temperature and precipitation and the negative but weak response of τ_{woo} to climate formed two compensatory forces that together contributed to the lower sensitivity of the τ_{veg} than of the τ_{soil} to climate.

Overall, τ_{veg} is widely perceived to be regulated primarily through stand dynamics, such as establishment, growth, self-thinning, and age-related mortality, and stochastic processes, such as management or disturbances (e.g., wildfires, frost damage, extreme drought, insects, and land use change; Ahlström et al., 2015; Allen et al., 2015; Anderegg et al., 2015; Erb et al., 2016; Thurner et al., 2016; Wang et al., 2018). These processes have complex and perhaps compensating interactions with climate. Climate change is then supposed to influence the frequency

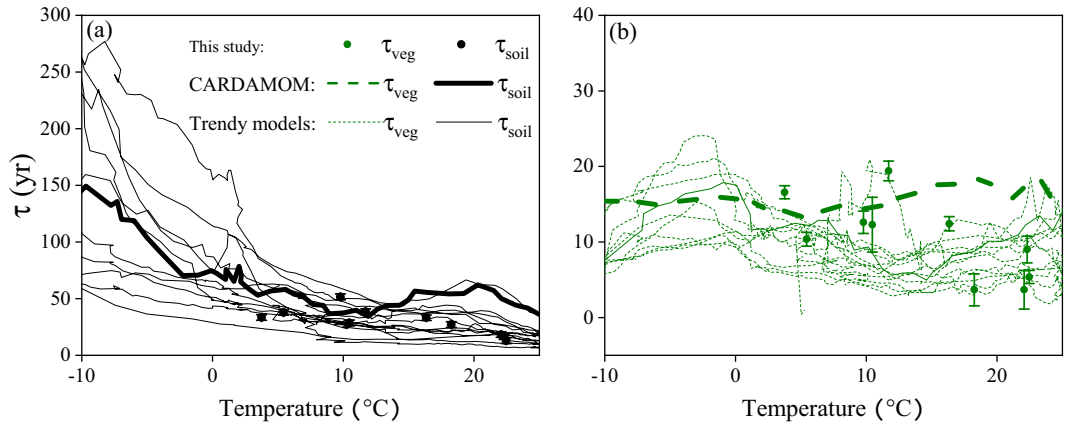

Figure 9. Associations of turnover times in soil τ_{soil}, (a) and vegetation τ_{veg}, (b) and with temperature calculated from CARDAMOM (thick line) and TRENDY (multiple fine lines representing various models) in the Northern Hemisphere. In comparison, the data from the present study are shown as solid points (mean value with 1 SE).

and severity of extreme climate events and thus potentially contributes to increased mortality rates. Accordingly, the biotic property, that is, vegetation age, rather than climatic factors, becomes the determinant for the τ_{veg} pattern (Figure 7a), especially in forest ecosystems (Wang et al., 2018). The effect of forest age on τ_{veg} helps explain the relatively weak response of τ_{veg} to climate.

4.3. Implications of the Various Climate Sensitivities of τ_{soil} and τ_{veg} for the Forest C Cycle

We quantified the various climate sensitivities of τ_{soil} and τ_{veg} and verified our findings against the MDF global benchmark derived from CARDAMOM and simulations of state-of-the-art LSMs from the TRENDY-v6 model set for the Northern Hemisphere; these comparisons all supported our findings of a higher climate sensitivity for τ_{soil} (Figure 9).The response to climate in the TRENDY models, especially in the soil pool, was highly variable (Figure 9). This variability is due to the poor constraint of C turnover times and its climatic response in current C cycle models (Anav et al., 2013; Braghiere et al., 2021; Friend et al., 2014; Terrer et al., 2021; Todd-Brown et al., 2013; Wieder et al., 2015); thus, whether the forest C sink can persist with global climate change remains largely unclear (Friedlingstein et al., 2014; Goodale et al., 2002). Our work is the first to constrain the various climate sensitivities of τ_{soil} and τ_{veg} via numerous long-term C cycle observations at realistic disequilibrium. The detailed sensitivity values and their differences at different PFTs can inform future forest modeling research. The higher climate sensitivities of τ_{soil} than τ_{veg} contributed to the varying pattern of τ_{diff}. The magnitude of τ_{diff} and the relationship of τ_{diff} with climate (Figures 4c and 4d) could be used as novel prior knowledge for ecological dynamic constraints in model-data assimilation (e.g., Bloom & Williams, 2015) or for model evaluation and development to reduce the uncertainties of these two key ecosystem traits, τ_{soil} and τ_{veg}.

Currently, the identification of the dynamics and distribution of forest C sequestration is a hot topic in C cycle research (Mckinley et al., 2011). In particular, forest soil C sequestration remains largely uncertain (Luyssaert et al., 2010; Pan et al., 2011). Quantifying highly uncertain ecosystem traits (e.g., C turnover times) and identifying their associations with soil C sequestration could yield a better understanding of the whole ecosystem C balance and its feedback to climate change. Here, we revealed that the difference between τ_{soil} and τ_{veg}, that is, τ_{diff}, could be a novel ecological indicator that is responsible for much of the variation in the capacity of C sequestration in soil. There was a significant decrease in the relative contribution of soil C sequestration with the decline in τ_{diff} under increasing temperature and precipitation. This decline in τ_{diff} was attributed primarily to the higher climate sensitivity of τ_{soil} than of τ_{veg}. To evaluate the robustness of this finding, we investigated not only the mean annual value of each site across climatic gradients but also the time-variant between annual values against climate change at each site. Both types of values revealed the higher climate sensitivity of τ_{soil} than of τ_{veg} (Figures S7 and S10 in Supporting Information S1), the lower τ_{diff} shortens in warmer and humid conditions (Figure S8 in Supporting Information S1), and accordingly, the lower contribution of ΔC_{dead} to NEP (Figure S9 in Supporting Information S1). The higher sensitivity of τ_{soil}/τ_{veg} in colder than warmer regions (Figure S10 in

Supporting Information S1) was well supported by Koven et al. (2017). Moreover, the overall temporal sensitivity of τ_{soil}/τ_{veg} to temperature (Figure S10 in Supporting Information S1, τ_{soil}: −1.34 years/°C, τ_{veg}: −0.53 years/°C) closely approximated the spatial sensitivity. The finding on the effect of various climate sensitivities of τ_{soil} and τ_{veg} on τ_{diff} and C sequestration has strong implications for the prediction of terrestrial C sink distributions in soil and vegetation under global warming and changes in precipitation regimes (IPCC, 2021). In addition, this knowledge can guide the implementation of C mitigation policies. Specifically, in the cold high-latitude region, substantial attention should be devoted to soil conservation since C is more strongly sequestered into soils; this consideration is especially important for permafrost soil with large amounts of organic C, which will be vulnerable to higher decomposition rates under rapid global warming (Koven et al., 2011). However, in warm and humid regions, we expect that more C will be sequestered in vegetation with increasing temperature and precipitation. For regional to global ecosystems with substantial young-aged afforestation under warm and humid conditions, for example, southern China, the total ecosystem C sink can be expected to be persistently enhanced due to the intrinsic age-structure effect on forest growth and the high relative contribution of the vegetation C sink (Fang et al., 2012; Yu et al., 2014).

Forest age affects the climate sensitivity of τ_{veg} and dominates the τ_{veg} pattern, which increases with increasing age (Wang et al., 2018); accordingly, in the present study, the difference between the τ_{veg} and τ_{soil} gradually shortened with forest age (Figure 7b). Since most old forests in this study are located in warmer and low-latitude regions, the age effect contributed to the negative relationships between τ_{diff} and climatic factors. Given the instinctive relationship between forest age and forest growth, for example, biomass accumulation and primary productivity (Goulden et al., 2011; Zaehle et al., 2006), we expect that improved representations of forest age-driven mortality into calibrated process-based models will better capture the climate responses of these highly uncertain traits, that is, τ_{veg} and τ_{veg}, and the age-structure-related effect on τ_{diff} and soil/vegetation C sequestration. In addition to forest age, the effect of climate on C cycling appeared to be indirectly mediated by nutrient availability. For example, nutrient availability (including the availability of nitrogen, phosphorous, and sulfur) plays a central role in the dynamic of both soil (Posada & Schuur, 2011; Torn et al., 2005) and vegetation (Gessler et al., 2017) C turnover, which was controlled to a large extent by nitrogen availability (Liang et al., 2019). Besides, current biogeochemical models usually lack microbial processes and thus miss an important feedback when considering the fate of C. Significantly different sensitivities have been highlighted between chemical modeling (with standard first-order kinetic representation of C decomposition) and biological modeling (with control of C decomposition through microbial activity) approaches for turnover process (Xenakis & Williams, 2014). Therefore, these mechanisms (e.g., C-nitrogen coupled cycling and interactions, and microbial activity) could be implemented in a model like DALEC and model-data fusion. These advances will help guide regional and global forest management and C mitigation efforts.

5. Conclusions

The present study provides the first quantification of the climate sensitivities of τ_{soil} and τ_{veg} and their differences at a realistic disequilibrium state. We gained insight into the mechanisms underlying the various climate sensitivities based on key C cycle process parameters: the opposite climate response between the woody allocation coefficient and woody turnover rate, the weaker climate sensitivity of plant mortality than of soil decomposition, and the strong age-structured effect on τ_{veg} together contributed to the lower climate sensitivity of τ_{veg} than of τ_{soil}. The various climate sensitivities of τ_{soil} and τ_{veg} determined the variation in τ_{diff}, which was revealed as an important indicator of the soil C sequestration capacity. The identification of the climate sensitivities of τ_{soil}/τ_{veg} and their effects on τ_{diff} and the relative contribution of soil C sequestration improves our understanding of C-climate feedback. Furthermore, the results of this study can facilitate the prediction of terrestrial C distribution in soil/vegetation under future climate change and guide both the implementation of C mitigation policies on forest plantations and soil conservation to dampen anthropogenic climate warming and help achieve C neutrality.

Conflict of Interest

The authors declare no conflicts of interest relevant to this study.

Data Availability Statement

The meteorological drivers, biomass, SOC, and LAI constraint data were all obtained from the CERN scientific and technological resources service system (http://www.cnern.org.cn/). The flux-tower NEE data used in this study were obtained at ChinaFLUX (http://www.chinaflux.org/general/). The data from this study have been deposited in a public data repository (https://figshare.com/s/cfb6efbde51ed79bc6e4).

Acknowledgments
This study was supported by the National Natural Science Foundation of China (Grant No. 42030509), the National Key Research and Development Program of China (Grant No. 2021YFF0703903), and the Strategic Priority Research Program of the Chinese Academy of Sciences (Grant No. XDA19020301). We thank the staff of CERN and ChinaFLUX for their dedication to observation and data processing. We thank Dr. Stephen Sitch (S.A.Sitch@exeter.ac.uk) for providing the TRENDY data (http://dgvm.ceh.ac.uk/). We also acknowledge the modeling groups and the TRENDY coordination team for their roles in producing and making available the TRENDY model output. MW acknowledges funding support from the Newton Fund CSSP, from the Royal Society, and UKSA Forests 2020.

References

Adams, H. D., Barron-Gafford, G. A., Minor, R. L., Gardea, A. A., Bentley, L. P., Law, D. J., et al. (2017). Temperature response surfaces for mortality risk of tree species with future drought. *Environmental Research Letters*, *12*(11), 115014. https://doi.org/10.1088/1748-9326/aa93be

Adams, H. D., Macalady, A. K., Breshears, D. D., Allen, C. D., Stephenson, N. L., Saleska, S. R., et al. (2010). Climate-induced tree mortality: Earth system consequences. *Eos, Transactions American Geophysical Union*, *91*(17), 153–154. https://doi.org/10.1029/2010EO170003

Ahlström, A., Xia, J., Arneth, A., Luo, Y., & Smith, B. (2015). Corrigendum: Importance of vegetation dynamics for future terrestrial carbon cycling (2015 environ. Res. lett.10 054019). *Environmental Research Letters*, *10*(5), 054019. https://doi.org/10.1088/1748-9326/10/5/054019

Allen, C. D., Breshears, D. D., & McDowell, N. G. (2015). On underestimation of global vulnerability to tree mortality and forest die-off from hotter drought in the Anthropocene. *Ecosphere*, *6*(8), 1–55. https://doi.org/10.1890/es15-00203.1

Allen, C. D., Macalady, A. K., Chenchouni, H., Bachelet, D., McDowell, N., Vennetier, M., et al. (2010). A global overview of drought and heat-induced tree mortality reveals emerging climate change risks for forests. *Forest Ecology and Management*, *259*(4), 660–684. https://doi.org/10.1016/j.foreco.2009.09.001

Anav, A. (2013). Evaluating the land and ocean components of the global carbon cycle in the cmip5 earth system models. *Journal of Climate*, *26*(18), 6801–6843. https://doi.org/10.1175/JCLI-D-12-00417.1

Anderegg, W. R., Flint, A., Huang, C. Y., Flint, L., Berry, J. A., Davis, F. W., et al. (2015). Tree mortality predicted from drought-induced vascular damage. *Nature Geoscience*, *8*(5), 367–371. https://doi.org/10.1038/ngeo2400

Bellassen, V., Delbart, N., Le Maire, G., Luyssaert, S., Ciais, P., & Viovy, N. (2011). Potential knowledge gain in large-scale simulations of forest carbon fluxes from remotely sensed biomass and height. *Forest Ecology and Management*, *261*(3), 515–530. https://doi.org/10.1016/j.foreco.2010.11.002

Bloom, A. A., Exbrayat, J. F., Ir, V. D. V., Feng, L., & Williams, M. (2016). The decadal state of the terrestrial carbon cycle: Global retrievals of terrestrial carbon allocation, pools, and residence times. *Proceedings of the National Academy of Sciences of the United States of America*, *113*(5), 172–173. https://doi.org/10.1073/pnas.1515160113

Bloom, A. A., & Williams, M. (2015). Constraining ecosystem carbon dynamics in a data-limited world: Integrating ecological "common sense" in a model-data fusion framework. *Biogeosciences*, *12*(5), 1299–1315. https://doi.org/10.5194/bg-12-1299-2015

Bradford, M. A., Wieder, W. R., Bonan, G. B., Fierer, N., Raymond, P. A., & Crowther, T. W. (2016). Managing uncertainty in soil carbon feedbacks to climate change. *Nature Climate Change*, *6*(8), 751–758. https://doi.org/10.1038/nclimate3071

Braghiere, R. K., Fisher, J. B., Fisher, R. A., Shi, M., Steidinger, B. S., Sulman, B. N., et al. (2021). Mycorrhizal distributions impact global patterns of carbon and nutrient cycling. *Geophysical Research Letters*, *48*, e2021GL094514. https://doi.org/10.1029/2021GL094514

Carvalhais, N., Forkel, M., Khomik, M., Bellarby, J., Jung, M., Migliavacca, M., et al. (2014). Global covariation of carbon turnover times with climate in terrestrial ecosystems. *Nature*, *514*(7521), 213–217. https://doi.org/10.1038/nature13731

Carvalhais, N., Reichstein, M., Ciais, P., Collatz, G. J., Mahecha, M. D., Montagnani, L., et al. (2010). Identification of vegetation and soil carbon pools out of equilibrium in a process model via eddy covariance and biometric constraints. *Global Change Biology*, *16*(10), 2813–2829. https://doi.org/10.1111/j.1365-2486.2010.02173.x

Carvalhais, N., Reichstein, M., Seixas, J., Collatz, G. J., Pereira, J. S., Berbigier, P., et al. (2008). Implications of the carbon cycle steady state assumption for biogeochemical modeling performance and inverse parameter retrieval. *Global Biogeochemical Cycles*, *22*, GB2007. https://doi.org/10.1029/2007gb003033

Chen, S., Huang, Y., Zou, J., & Shi, Y. (2013). Mean residence time of global topsoil organic carbon depends on temperature, precipitation and soil nitrogen. *Global and Planetary Change*, *100*, 99–108. https://doi.org/10.1016/j.gloplacha.2012.10.006

Conant, R. T., Ryan, M. G., Ågren, G. I., Birge, H. E., Davidson, E. A., Eliasson, P. E., et al. (2011). Temperature and soil organic matter decomposition rates—Synthesis of current knowledge and a way forward. *Global Change Biology*, *17*(11), 3392–3404. https://doi.org/10.1111/j.1365-2486.2011.02496.x

Craine, J. M., Fierer, N., & McLauchlan, K. K. (2010). Widespread coupling between the rate and temperature sensitivity of organic matter decay. *Nature Geoscience*, *3*, 854–857. https://doi.org/10.1038/ngeo1009

Davidson, E. A., & Janssens, I. A. (2006). Temperature sensitivity of soil carbon decomposition and feedbacks to climate change. *Nature*, *440*, 165–173. https://doi.org/10.1038/nature04514

De Kauwe, M. G., Medlyn, B. E., Zaehle, S., Walker, A. P., Dietze, M. C., Wang, Y. P., et al. (2014). Where does the carbon go? A model–data intercomparison of vegetation carbon allocation and turnover processes at two temperate forest free-air CO_2 enrichment sites. *New Phytologist*, *203*(3), 883–899. https://doi.org/10.1111/nph.12847

Dietze, M. C., Fox, A., Beck-Johnson, L. M., Betancourt, J. L., Hooten, M. B., Jarnevich, C. S., et al. (2018). Iterative near-term ecological forecasting: Needs, opportunities, and challenges. *Proceedings of the National Academy of Sciences of the United States of America*, *115*(7), 1424–1432. https://doi.org/10.1073/pnas.1710231115

Erb, K. H., Fetzel, T., Plutzar, C., Kastner, T., Lauk, C., Mayer, A., et al. (2016). Biomass turnover time in terrestrial ecosystems halved by land use. *Nature Geoscience*, *9*(9), 674. https://doi.org/10.1038/ngeo2782

Exbrayat, J. F., Pitman, A. J., & Abramowitz, G. (2014). Response of microbial decomposition to spin-up explains CMIP5 soil carbon range until 2100. *Geoscientific Model Development*, *7*(6), 2683–2692. https://doi.org/10.5194/gmd-7-2683-2014

Famiglietti, C. A., Smallman, T. L., Levine, P. A., Flack-Prain, S., Quetin, G. R., Meyer, V., et al. (2021). Optimal model complexity for terrestrial carbon cycle prediction. *Biogeosciences*, *18*(8), 2727–2754. https://doi.org/10.5194/bg-18-2727-2021

Fan, N., Koirala, S., Reichstein, M., Thurner, M., Avitabile, V., Santoro, M., et al. (2020). Apparent ecosystem carbon turnover time: Uncertainties and robust features. *Earth System Science Data*, *12*(4), 2517–2536. https://doi.org/10.5194/essd-12-2517-2020

Fang, J., Shen, Z., Tang, Z., Wang, X., Wang, Z., Feng, J., et al. (2012). Forest community survey and the structural characteristics of forests in China. *Ecography*, *35*(12), 1059–1071. https://doi.org/10.1111/j.1600-0587.2013.00161.x

Fox, A., Williams, M., Richardson, A. D., Cameron, D., Gove, J. H., Quaife, T., et al. (2009). The REFLEX project: Comparing different algorithms and implementations for the inversion of a terrestrial ecosystem model against eddy covariance data. *Agricultural and Forest Meteorology*, *149*(10), 1597–1615. https://doi.org/10.1016/j.agrformet.2009.05.002

Friend, A. D., Lucht, W., Rademacher, T. T., Keribin, R., Betts, R., Cadule, P., et al. (2014). Carbon residence time dominates uncertainty in terrestrial vegetation responses to future climate and atmospheric co2. *Proceedings of the National Academy of Sciences of the United States of America*, *111*(9), 3280. https://doi.org/10.1073/pnas.1222477110

Friedlingstein, P., Meinshausen, M., Arora, V. K., Jones, C. D., Anav, A., Liddicoat, S. K., et al. (2014). Uncertainties in CMIP5 climate projections due to carbon cycle feedbacks. *Journal of Climate*, *27*(2), 511–526. https://doi.org/10.1175/jcli-d-12-00579.1

Fu, B. J., Li, S. G., Yu, X. B., Yang, P., Yu, G. R., Feng, R. G., et al. (2010). Chinese ecosystem research network: Progress and perspectives. *Ecological Complexity*, *7*, 225–233. https://doi.org/10.1016/j.ecocom.2010.02.007

Galbraith, D., Malhi, Y., Affum-Baffoe, K., Castanho, A. D., Doughty, C. E., Fisher, R. A., et al. (2013). Residence times of woody biomass in tropical forests. Plant Ecology & *Diversity*, *6*(1), 139–157. https://doi.org/10.1080/17550874.2013.770578

Ge, R., He, H., Ren, X., Zhang, L., Yu, G., Smallman, T. L., et al. (2019). Underestimated ecosystem carbon turnover time and sequestration under the steady state assumption: A perspective from long-term data assimilation. *Global Change Biology*, *25*(3), 938–953. https://doi.org/10.1111/gcb.14547

Gessler, A., Schaub, M., & McDowell, N. G. (2017). The role of nutrients in drought-induced tree mortality and recovery. *New Phytologist*, *214*(2), 513–520. https://doi.org/10.1111/nph.14340

Goodale, C. L., Apps, M. J., Birdsey, R. A., Field, C. B., Heath, L. S., Houghton, R. A., et al. (2002). Forest carbon sinks in the northern hemisphere. *Ecological Applications*, *12*, 891–899. https://doi.org/10.1890/1051-0761(2002)012[0891:FCSITN]2.0.CO;2

Goulden, M. L., McMillan, A. M. S., Winston, G. C., Rocha, A. V., Manies, K. L., Harden, J. W., & Bond-Lamberty, B. P. (2011). Patterns of NPP, GPP, respiration, and NEP during boreal forest succession. *Global Change Biology*, *17*(2), 855–871. https://doi.org/10.1111/j.1365-2486.2010.02274.x

Guillemot, J., Martin-StPaul, N. K., Dufrêne, E., François, C., Soudani, K., Ourcival, J. M., & Delpierre, N. (2015). The dynamic of the annual carbon allocation to wood in European tree species is consistent with a combined source–sink limitation of growth: Implications for modelling. *Biogeosciences*, *12*(9), 2773–2790. https://doi.org/10.5194/bg-12-2773-2015

He, Y., Trumbore, S. E., Torn, M. S., Harden, J. W., Vaughn, L. J., Allison, S. D., et al. (2016). Radiocarbon constraints imply reduced carbon uptake by soils during the 21st century. *Science*, *353*(6306), 1419–1424. https://doi.org/10.1126/science.aad4273

Heckman, K., Throckmorton, H., Clingensmith, C., Vila, F. J. G., Horwath, W. R., Knicker, H., et al. (2014). Factors affecting the molecular structure and mean residence time of occluded organics in a lithosequence of soils under ponderosa pine. *Soil Biology and Biochemistry*, *77*, 1–11. https://doi.org/10.1016/j.soilbio.2014.05.028

Hurtt, G. C., & Armstrong, R. A. (1996). A pelagic ecosystem model calibrated with BATS data. *Deep Sea Research Part II: Topical Studies in Oceanography*, *43*(2–3), 653–683. https://doi.org/10.1016/0967-0645(96)00007-0

IPCC. (2021). Climate change 2021: The physical science basis. In A.Pirani, S. L.Connors, C.Péan, S.Berger, V. Masson-delmotte, P. Zhai, et al. (Eds.), *Contribution of working group I to the Sixth Assessment Report of the Intergovernmental Panel on climate change. Summary for policymakers*. Cambridge University Press.

Knorr, W., Prentice, I. C., House, J. I., & Holland, E. A. (2005). Long-term sensitivity of soil carbon turnover to warming. *Nature*, *433*, 298–301. https://doi.org/10.1038/nature03226

Koven, C. D., Chambers, J. Q., Georgiou, K., Knox, R., Negron-Juarez, R., Riley, W. J., et al. (2015). Controls on terrestrial carbon feedbacks by productivity versus turnover in the CMIP5 Earth System Models. *Biogeosciences*, *12*(17), 5211–5228. https://doi.org/10.5194/bg-12-5211-2015

Koven, C. D., Hugelius, G., Lawrence, D. M., & Wieder, W. R. (2017). Higher climatological temperature sensitivity of soil carbon in cold than warm climates. *Nature Climate Change*, *7*(11), 817–822. https://doi.org/10.1038/nclimate3421

Koven, C. D., Ringeval, B., Friedlingstein, P., Ciais, P., Cadule, P., Khvorostyanov, D., et al. (2011). Permafrost carbon-climate feedbacks accelerate global warming. *Proceedings of the National Academy of Sciences of the United States of America*, *108*(36), 14769–14774. https://doi.org/10.1073/pnas.1103910108

LeBauer, D. S., Wang, D., Richter, K. T., Davidson, C. C., & Dietze, M. C. (2013). Facilitating feedbacks between field measurements and ecosystem models. *Ecological Monographs*, *83*(2), 133–154. https://doi.org/10.1890/12-0137.1

Le Quéré, C., Andrew, R. M., Friedlingstein, P., Sitch, S., Pongratz, J., Manning, A. C., et al. (2018). Global carbon Budget 2017. *Earth System Science Data*, *10*(1), 405–448.

Liang, Z., Olesen, J. E., Jensen, J. L., & Elsgaard, L. (2019). Nutrient availability affects carbon turnover and microbial physiology differently in topsoil and subsoil under a temperate grassland. *Geoderma*, *336*, 22–30. https://doi.org/10.1016/j.geoderma.2018.08.021

López-Blanco, E., Exbrayat, J. F., Lund, M., Christensen, T. R., Tamstorf, M. P., Slevin, D., et al. (2019). Evaluation of terrestrial pan-Arctic carbon cycling using a data-assimilation system. *Earth System Dynamics*, *10*(2), 233–255.

Luo, Y., Ahlström, A., Allison, S. D., Batjes, N. H., Brovkin, V., Carvalhais, N., et al. (2016). Toward more realistic projections of soil carbon dynamics by earth system models. *Global Biogeochemical Cycles*, *30*, 40–56. https://doi.org/10.1002/2015GB005239

Luo, Y., Shi, Z., Lu, X., Xia, J., Liang, J., Jiang, J., et al. (2017). Transient dynamics of terrestrial carbon storage: Mathematical foundation and numeric examples. *Biogeosciences*, *14*(1), 145–161. https://doi.org/10.5194/bg-14-145-2017

Luo, Y., & Weng, E. (2011). Dynamic disequilibrium of the terrestrial carbon cycle under global change. *Trends in Ecology & Evolution*, *26*(2), 96–104. https://doi.org/10.1016/j.tree.2010.11.003

Luo, Y., White, L. W., Canadell, J. G., DeLucia, E. H., Ellsworth, D. S., Finzi, A., et al. (2003). Sustainability of terrestrial carbon sequestration: A case study in Duke forest with inversion approach. *Global Biogeochemical Cycles*, *17*(1), 1021. https://doi.org/10.1029/2002GB001923

Luo, Z., Wang, G., & Wang, E. (2019). Global subsoil organic carbon turnover times dominantly controlled by soil properties rather than climate. *Nature Communications*, *10*(1), 1–10. https://doi.org/10.1038/s41467-019-11597-9

Luyssaert, S., Ciais, P., Piao, S. L., Schulze, E. D., Jung, M., Zaehle, S., et al. (2010). The European carbon balance. Part 3: Forests. *Global Change Biology*, *16*(5), 1429–1450. https://doi.org/10.1111/j.1365-2486.2009.02056.x

Mahecha, M. D., Reichstein, M., Carvalhais, N., Lasslop, G., Lange, H., Seneviratne, S. I., et al. (2010). Global convergence in the temperature sensitivity of respiration at ecosystem level. *Science*, *329*(5993), 838–840. https://doi.org/10.1126/science.1189587

Malhi, Y., Baker, T. R., Phillips, O. L., Almeida, S., Alvarez, E., Arroyo, L., et al. (2004). The above-ground coarse wood productivity of 104 Neotropical forest plots. *Global Change Biology*, *10*(5), 563–591. https://doi.org/10.1111/j.1529-8817.2003.00778.x

Malhi, Y., Saatchi, S., Girardin, C., & Aragaˆo, L. E. O. C. (2009). The production, storage, and flow of carbon in Amazonian forests. In M.Keller, M.Bustamante, J.Gash, & P.Silva Dias (Eds.), *Amazonia and global change* (Vol. 186, pp. 355–372). American Geophysical Union.

Mcdowell, N. G., Williams, A. P., Xu, C., Pockman, W. T., Dickman, L. T., Sevanto, S., et al. (2016). Multi-scale predictions of massive conifer mortality due to chronic temperature rise. *Nature Climate Change*, *6*(3), 295. https://doi.org/10.1038/nclimate2873

McKinley, D. C., Ryan, M. G., Birdsey, R. A., Giardina, C. P., Harmon, M. E., Heath, L. S., et al (2011). A synthesis of current knowledge on forests and carbon storage in the United States. *Ecological Applications*, *21*, 1902–1924. https://doi.org/10.1890/10-0697.1

Metropolis, N., Rosenbluth, A. W., Rosenbluth, M. N., Teller, A. H., & Teller, E. (1953). Equation of state calculations by fast computing machines. *The Journal of Chemical Physics*, *21*(6), 1087–1092. https://doi.org/10.1063/1.1699114

Meyer, N., Welp, G., & Amelung, W. (2018). The temperature sensitivity (Q10) of soil respiration: Controlling factors and spatial prediction at regional scale based on environmental soil classes. *Global Biogeochemical Cycles*, *32*, 306–323. https://doi.org/10.1002/2017GB005644

Norton, A. J., Rayner, P. J., Koffi, E. N., Scholze, M., Silver, J. D., & Wang, Y.-P. (2019). Estimating global gross primary productivity using chlorophyll fluorescence and a data assimilation system with the BETHY-SCOPE model. *Biogeosciences*, *16*(15), 3069–3093. https://doi.org/10.5194/bg-16-3069-2019

Pan, Y. D., Birdsey, R. A., Fang, J. Y., Houghton, R., Kauppi, P. E., Kurz, W. A., et al. (2011). A large and persistent carbon sink in the world's forests. *Science*, *333*, 988–993. https://doi.org/10.1126/science.1201609

Peylin, P., Bacour, C., MacBean, N., Leonard, S., Rayner, P., Kuppel, S., et al. (2016). A new stepwise carbon cycle data assimilation system using multiple data streams to constrain the simulated land surface carbon cycle. *Geoscientific Model Development*, *9*(9), 3321–3346. https://doi.org/10.5194/gmd-9-3321-2016

Piao, S., Luyssaert, S., Ciais, P., Janssens, I. A., Chen, A., Cao, C., et al. (2010). Forest annual carbon cost: A global-scale analysis of autotrophic respiration. *Ecology*, *91*(3), 652–661. https://doi.org/10.1890/08-2176.1

Posada, J. M., & Schuur, E. A. (2011). Relationships among precipitation regime, nutrient availability, and carbon turnover in tropical rain forests. *Oecologia*, *165*(3), 783–795. https://doi.org/10.1007/s00442-010-1881-0

Quesada, C. A., Phillips, O. L., Schwarz, M., Czimczik, C. I., Baker, T. R., Patiño, S., et al. (2012). Basin-wide variations in Amazon forest structure and function are mediated by both soils and climate. *Biogeosciences*, *9*(6), 2203–2246. https://doi.org/10.5194/bg-9-2203-2012

Quetin, G. R., Bloom, A. A., Bowman, K. W., & Konings, A. G. (2020). Carbon flux variability from a relatively simple ecosystem model with assimilated data is consistent with terrestrial biosphere model estimates. *Journal of Advances in Modeling Earth Systems*, *12*, e2019MS001889. https://doi.org/10.1029/2019MS001889

Reichstein, M., Bahn, M., Ciais, P., Frank, D., Mahecha, M. D., Seneviratne, S. I., et al. (2013). Climate extremes and the carbon cycle. *Nature*, *500*(7462), 287–295. https://doi.org/10.1038/nature12350

Schimel, D. S., Braswell, B. H., Holland, E. A., McKeown, R., Ojima, D. S., Painter, T. H., et al. (1994). Climatic, edaphic, and biotic controls over storage and turnover of carbon in soils. *Global Biogeochemical Cycles*, *8*(3), 279–293. https://doi.org/10.1029/94GB00993

Schmidt, M. W. I., Torn, M. S., Abiven, S., Dittmar, T., Guggenberger, G., Janssens, I. A., et al. (2011). Persistence of soil organic matter as an ecosystem property. *Nature*, *478*, 49–56. https://doi.org/10.1038/nature10386

Schwalm, C. R., Huntzinger, D. N., Michalak, A. M., Schaefer, K., Fisher, J. B., Fang, Y., & Wei, Y. (2020). Modeling suggests fossil fuel emissions have been driving increased land carbon uptake since the turn of the 20th Century. *Scientific Reports*, *10*(1), 9059. https://doi.org/10.1038/s41598-020-66103-9

Schwartz, S. E. (1979). Residence times in reservoirs under non-steady-state conditions: Application to atmospheric so2 and aerosol sulfate1. *Tellus*, *31*(6), 530–547. https://doi.org/10.3402/tellusa.v31i6.10471

Shiklomanov, A. N., Bond-Lamberty, B., Atkins, J. W., & Gough, C. M. (2020). Structure and parameter uncertainty in centennial projections of forest community structure and carbon cycling. *Global Change Biology*, *26*(11), 6080–6096. https://doi.org/10.1111/gcb.15164

Sierra, C. A., Trumbore, S. E., Davidson, E. A., Vicca, S., & Janssens, I. (2015). Sensitivity of decomposition rates of soil organic matter with respect to simultaneous changes in temperature and moisture. *Journal of Advances in Modeling Earth Systems*, *7*, 335–356. https://doi.org/10.1002/2014MS000358

Sitch, S., Friedlingstein, P., Gruber, N., Jones, S. D., Murray-Tortarolo, G., Ahlström, A., et al. (2015). Recent trends and drivers of regional sources and sinks of carbon dioxide. *Biogeosciences*, *12*(3), 653–679. https://doi.org/10.5194/bg-12-653-2015

Sitch, S., Smith, B., Prentice, I. C., Arneth, A., Bondeau, A., Cramer, W., et al. (2003). Evaluation of ecosystem dynamics, plant geography and terrestrial carbon cycling in the LPJ dynamic global vegetation model. *Global Change Biology*, *9*(2), 161–185. https://doi.org/10.1046/j.1365-2486.2003.00569.x

Slevin, D., Tett, S. F., Exbrayat, J. F., Bloom, A. A., & Williams, M. (2016). Global evaluation of gross primary productivity in the JULES land surface model v3. 4.1. *Geoscientific Model Development*, *10*(7), 2651–2670.

Smallman, T. L., Exbrayat, J. F., Mencuccini, M., Bloom, A. A., & Williams, M. (2017). Assimilation of repeated woody biomass observations constrains decadal ecosystem carbon cycle uncertainty in aggrading forests. *Journal of Geophysical Research: Biogeosciences*, *122*, 528–545. https://doi.org/10.1002/2016JG003520

Smallman, T. L., & Mathew, W. (2019). Description and validation of an intermediate complexity model for ecosystem photosynthesis and evapotranspiration: ACM-GPP-ETv1. *Geoscientific Model Development*, *12*, 2227–2253. https://doi.org/10.5194/gmd-12-2227-2019

Smith, M. J., Purves, D. W., Vanderwel, M. C., Lyutsarev, V., & Emmott, S. (2013). The climate dependence of the terrestrial carbon cycle, including parameter and structural uncertainties. *Biogeosciences*, *10*(1), 583–606. https://doi.org/10.5194/bg-10-583-2013

Song, X., Zeng, X., & Tian, D. (2018). Allocation of forest net primary production varies by forest age and air temperature. *Ecology and Evolution*, *8*(23), 12163–12172. https://doi.org/10.1002/ece3.4675

Terrer, C., Phillips, R. P., Hungate, B. A., Rosende, J., Pett-Ridge, J., Craig, M. E., et al. (2021). A trade-off between plant and soil carbon storage under elevated CO2. *Nature*, *591*(7851), 599–603. https://doi.org/10.1038/s41586-021-03306-8

Thomsen, I. K., Schjønning, P., Jensen, B., Kirstensen, K., & Christensen, B. T. (1999). Turnover of organic matter in different texture soils. II. Microbial activity as influenced by soil water regimes. *Geoderma*, *89*, 199–218. https://doi.org/10.1016/s0016-7061(98)00084-6

Thurner, M., Beer, C., Carvalhais, N., Forkel, M., Santoro, M., Tum, M., et al. (2016). Large-scale variation in boreal and temperate forest carbon turnover rate related to climate. *Geophysical Research Letters*, *43*, 4576–4585. https://doi.org/10.1002/2016GL068794

Thurner, M., Beer, C., Ciais, P., Friend, A. D., Ito, A., Kleidon, A., et al. (2017). Evaluation of climate-related carbon turnover processes in global vegetation models for boreal and temperate forests. *Global Change Biology*, *23*(8), 3076–3091. https://doi.org/10.1111/gcb.13660

Todd-Brown, K. E. O., Randerson, J. T., Hopkins, F., Arora, V., Hajima, T., Jones, C., et al. (2014). Changes in soil organic carbon storage predicted by earth system models during the 21st century. *Biogeosciences*, *10*(12), 18969–19004. https://doi.org/10.5194/bg-11-2341-2014

Todd-Brown, K. E. O., Randerson, J. T., Post, W. M., Hoffman, F. M., Tarnocai, C., Schuur, E. A. G., et al. (2013). Causes of variation in soil carbon simulations from CMIP5 Earth system models and comparison with observations. *Biogeosciences*, *10*(13), 1717–1736. https://doi.org/10.5194/bg-10-1717-2013

Torn, M. S., Vitousek, P. M., & Trumbore, S. E. (2005). The influence of nutrient availability on soil organic matter turnover estimated by incubations and radiocarbon modeling. *Ecosystems*, *8*(4), 352–372. https://doi.org/10.1007/s10021-004-0259-8

Trumbore, S. (2000). Age of soil organic matter and soil respiration: Radiocarbon constraints on belowground C dynamics. *Ecological Applications*, *10*(2), 399–411. https://doi.org/10.1890/1051-0761(2000)010[0399:AOSOMA]2.0.CO;2

Trumbore, S. (2006). Carbon respired by terrestrial ecosystems—Recent progress and challenges. *Global Change Biology*, *12*(2), 141–153. https://doi.org/10.1111/j.1365-2486.2006.01067.x

Trumbore, S. E., Chadwick, O. A., & Amundson, R. (1996). Rapid exchange between soil carbon and atmospheric carbon dioxide driven by temperature change. *Science*, *272*(5260), 393–396. https://doi.org/10.1126/science.272.5260.393

Wang, J., Sun, J., Xia, J., He, N., Li, M., & Niu, S. (2018). Soil and vegetation carbon turnover times from tropical to boreal forests. *Functional Ecology*, *32*(1), 71–82. https://doi.org/10.1111/1365-2435.12914

Wang, J., Sun, J., Yu, Z., Li, Y., Tian, D., Wang, B., et al. (2019). Vegetation type controls root turnover in global grasslands. *Global Ecology and Biogeography*, *28*(4), 442–455. https://doi.org/10.1111/geb.12866

White, E. P., Yenni, G. M., Taylor, S. D., Christensen, E. M., Bledsoe, E. K., Simonis, J. L., et al. (2019). Developing an automated iterative near-term forecasting system for an ecological study. *Methods in Ecology and Evolution*, *10*(3), 332–344. https://doi.org/10.1111/2041-210x.13104

Wieder, W. R., Cleveland, C. C., Smith, W. K., & Todd-Brown, K. (2015). Future productivity and carbon storage limited by terrestrial nutrient availability. *Nature Geoscience*, *8*, 441–444. https://doi.org/10.1038/ngeo2413

Williams, A. P., Allen, C. D., Macalady, A. K., Griffin, D., Woodhouse, C. A., Meko, D. M., et al. (2013). Temperature as a potent driver of regional forest drought stress and tree mortality. *Nature Climate Change*, *3*(3), 292–297. https://doi.org/10.1038/nclimate1693

Williams, M., Schwarz, P. A., Law, B. E., Irvine, J., & Kurpius, M. R. (2005). An improved analysis of forest carbon dynamics using data assimilation. *Global Change Biology*, *11*(1), 89–105. https://doi.org/10.1111/j.1365-2486.2004.00891.x

Wu, D., Piao, S., Liu, Y., Ciais, P., & Yao, Y. (2018). Evaluation of CMIP5 Earth System Models for the spatial patterns of biomass and soil carbon turnover times and their linkage with climate. *Journal of Climate*, *31*(15), 5947–5960. https://doi.org/10.1175/jcli-d-17-0380.1

Wu, D., Piao, S., Zhu, D., Wang, X., Ciais, P., Bastos, A., et al. (2020). Accelerated terrestrial ecosystem carbon turnover and its drivers. *Global Change Biology*, *26*(9), 5052–5062. https://doi.org/10.1111/gcb.15224

Wu, G., Cai, X., Keenan, T. F., Li, S., Luo, X., Fisher, J. B., et al. (2020). Evaluating three evapotranspiration estimates from model of different complexity over China using the ILAMB benchmarking system. *Journal of Hydrology*, *590*, 125553. https://doi.org/10.1016/j.jhydrol.2020.125553

Xenakis, G., & Williams, M. (2014). Comparing microbial and chemical kinetics for modelling soil organic carbon decomposition using the DecoChem v1. 0 and DecoBio v1. 0 models. *Geoscientific Model Development*, *7*(4), 1519–1533. https://doi.org/10.5194/gmd-7-1519-2014

Xia, J., Chen, Y., Liang, S., Liu, D., & Yuan, W. (2015). Global simulations of carbon allocation coefficients for deciduous vegetation types. *Tellus Series B Chemical and Physical Meteorology*, *67*(2), 59–81. https://doi.org/10.3402/tellusb.v67.28016

Xue, B. L., Guo, Q., Hu, T., Xiao, J., Yang, Y., Wang, G., et al. (2017). Global patterns of woody residence time and its influence on model simulation of aboveground biomass. *Global Biogeochemical Cycles*, *31*, 821–835. https://doi.org/10.1002/2016GB005557

Yan, Y., Luo, Y., Zhou, X., & Chen, J. (2014). Sources of variation in simulated ecosystem carbon storage capacity from the 5th climate model intercomparison project (cmip5). *Tellus Series B Chemical and Physical Meteorology*, *66*(1), 92–109. https://doi.org/10.3402/tellusb.v66.22568

Yan, Y., Zhou, X., Jiang, L., & Luo, Y. (2017). Effects of carbon turnover time on terrestrial ecosystem carbon storage. *Biogeosciences*, *14*(23), 5441. https://doi.org/10.5194/bg-14-5441-2017

Yu, G., Chen, Z., Piao, S., Peng, C., Ciais, P., Wang, Q., et al. (2014). High carbon dioxide uptake by subtropical forest ecosystems in the East Asian monsoon region. *Proceedings of the National Academy of Sciences of the United States of America*, *111*(13), 4910–4915. https://doi.org/10.1073/pnas.1317065111

Yu, K., Smith, W. K., Trugman, A. T., Condit, R., Hubbell, S. P., Sardans, J., et al. (2019). Pervasive decreases in living vegetation carbon turnover time across forest climate zones. *Proceedings of the National Academy of Sciences of the United States of America*, *116*(49), 24662–24667. https://doi.org/10.1073/pnas.1821387116

Zaehle, S., Sitch, S., Prentice, I. C., Liski, J., Cramer, W., Erhard, M., et al. (2006). The importance of age-related decline in forest NPP for modeling regional carbon balances. *Ecological Applications*, *16*(4), 1555–1574. https://doi.org/10.1890/1051-0761(2006)016[1555:TIOADI]2.0.CO;2

Zhang, L., Luo, Y., Yu, G., & Zhang, L. (2010). Estimated carbon residence times in three forest ecosystems of eastern China: Applications of probabilistic inversion. *Journal of Geophysical Research*, *115*, G01010. https://doi.org/10.1029/2009JG001004

Zheng, Z. M., Yu, G. R., Sun, X. M., Li, S. G., Wang, Y. S., Wang, Y. H., et al. (2010). Spatio-temporal variability of soil respiration of forest ecosystems in China: Influencing factors and evaluation model. *Environmental Management*, *46*(4), 633–642. https://doi.org/10.1007/s00267-010-9509-z

Zhou, G., Liu, S., Li, Z., Zhang, D., Tang, X., Zhou, C., et al. (2006). Old-growth forests can accumulate carbon in soils. *Science*, *314*(5804), 1417. https://doi.org/10.1126/science.1130168

Zhou, T., & Luo, Y. (2008). Spatial patterns of ecosystem carbon residence time and NPP-driven carbon uptake in the conterminous United States. *Global Biogeochemical Cycles*, *22*, GB3032. https://doi.org/10.1029/2007GB002939

Zhou, T., Shi, P., Hui, D., & Luo, Y. (2009). Global pattern of temperature sensitivity of soil heterotrophic respiration (Q10) and its implications for carbon-climate feedback. *Journal of Geophysical Research*, *114*, G02016. https://doi.org/10.1029/2008JG000850

Zhou, T., Shi, P., Jia, G., & Luo, Y. (2013). Nonsteady state carbon sequestration in forest ecosystems of China estimated by data assimilation. *Journal of Geophysical Research: Biogeosciences*, *118*, 1369–1384. https://doi.org/10.1002/jgrg.20114

Zhou, X., Zhou, T., & Luo, Y. (2012). Uncertainties in carbon residence time and NPP-driven carbon uptake in terrestrial ecosystems of the conterminous USA: A Bayesian approach. *Tellus B: Chemical and Physical Meteorology*, *64*(1), 577–583. https://doi.org/10.3402/tellusb.v64i0.17223